

Compressional and Shear Wave Velocities in South Island, New Zealand Rocks and Their Application to the Interpretation of Seismological Models of the New Zealand Crust

Nikolas I. Christensen

*Department of Geology and Geophysics, University of Wisconsin-Madison, Madison, Wisconsin
and Department of Earth and Ocean Sciences, University of British Columbia, Vancouver, Canada*

David A. Okaya

Department of Earth Sciences, University of Southern California, Los Angeles, California

The seismic properties of a suite of metamorphic and igneous rocks from South Island, New Zealand have been investigated using laboratory velocity measurements as a function of confining pressures up to 1000 MPa. Representative samples for the velocity measurements were collected from the Caples, Aspiring, Torlesse, Buller, and Takaka Terranes. Lithologies studied include quartzofeldspathic schists, amphibolites, greenschists, slates, argillites, graywackes, gabbros and granites. Seismic velocities, in general, increase with increasing density. Whole rock geochemical analyses show velocities increase with decreasing SiO₂ contents. Compressional wave velocities increase with increasing Mg numbers for Haast Schist and Torlesse samples, however velocities of the Haast schist rocks do not show any correlation with metamorphic grade. Haast schists are highly anisotropic due to preferred mineral orientations, whereas the Torlesse greywackes are isotropic. Symmetry of the anisotropic rocks varies from axial to orthorhombic, with fast compressional wave velocities parallel to lineations. Shear wave splitting is only significant for propagation directions at high angles to foliation normals; minimal production at other angles can mistakenly be interpreted as due to isotropic media. A refraction experiment shot in orthogonal directions across the Haast Schist shows 6% compressional wave anisotropy, in good agreement with the laboratory measurements. We conclude that seismic anisotropy is a pervasive feature throughout much of the South Island crust.

INTRODUCTION

For interpreting structures modeled by seismic experiments, which are based on P-wave and S-wave velocities, a systematic data base of velocities for appropriate rock types are required with a precision at least comparable with that of seismological measurements. In particular, for continental crustal studies we require velocity measurements under conditions approaching 30 to 50 km depths. Of fundamental importance

is the role of pressure which increases with depth and reaches about 1000 MPa at 35 km. In this paper we present a database of compressional and shear wave velocities for a wide variety of South Island, New Zealand rocks at hydrostatic confining pressures to 1000 MPa. The measurements were part of the joint USA-New Zealand geophysical study of the continent-continent transform plate boundary in South Island, New Zealand, which separates the Australian and Pacific plates. In the following sections emphasis is placed on the correlation of seismic velocities with various physical and chemical parameters, with the goal of interpreting field studies of seismic velocities of South Island, New Zealand.

SAMPLE LOCALITIES

The physical property measurements encompass rocks from several tectonostratigraphic terranes of South Island New Zealand. Based on the classifications of *Bishop et al.* [1985] and *Frost and Coombs* [1989] these include samples from the Buller and Takaka terranes of the Western Province and the Murihiku, Caples, Aspiring and older Torlesse terranes of the Eastern Province (Plate 1). These papers provide detailed information on the ages, lithologies, and tectonic settings of the various terranes; additional information is available in *Cox and Sutherland* [this volume]. Much of the following discussion focuses on seismic properties of rocks from the Caples, Aspiring and Torlesse terranes, since the majority of the samples were collected from these terranes and recent seismic studies have targeted these regions. The rocks are primarily quartzofeldspathic schists, greywackes, argillites and mafic volcanics, which have been subjected to zeolite, greenschist and higher grade metamorphism (Table 1).

The rocks selected for this study were collected during the South Island Geophysical Transect [e.g., *Davey et al.*, this volume] from several major South Island localities representing Alpine and Otago schists, the Alpine fault zone, Torlesse greywacke, Tuhua granite, Fiordland gabbro and Murihiku greywacke and argillite (Plate 1). All samples were collected in place from outcrops, except the jadestone (A-26) and garnet amphibolite (A-79) which were collected as float.

EXPERIMENTAL PROCEDURES

The new measurements are based on a pulse transmission technique described by *Birch* [1960]. To investigate anisotropy, three cores, 2.54 cm in diameter and 5–8 cm in length, were cut with mutually perpendicular axes from all specimens. Using specially designed sample holders and protractors, the cores were taken to within a few degrees of the desired directions. A-cores were taken normal to foliations and either B or C-cores were cut parallel to lineations, when

present. Velocities were measured in all samples at room temperature with both rising and descending pressure at 20 MPa intervals for confining pressures between 0 and 100 MPa, at 50 MPa intervals between 100 and 200 MPa, and at 100 MPa intervals between 200 and 1000 MPa. Compressional and shear waves were generated across each sample by means of lead-zirconate-titanate (PZT) and AC-cut quartz transducers, respectively, having resonant frequencies of 2 MHz. Vibration directions for the shear wave A-core velocity measurements were oriented parallel to the B-core axes. For foliated rocks, B-core vibration directions were parallel to foliations and C-core vibration directions were normal to foliations. Thus for transversely isotropic samples, comparisons of B and C-core shear wave velocities are a measure of shear wave splitting for propagation within the foliation. Compressional and shear wave velocity data, together with V_p/V_s and Poisson's ratios calculated from mean velocities are presented in Table 2 for ten pressures up to 1000 MPa. The cumulative error limits for compressional and shear wave velocities are estimated to be 0.5% and 1.0% respectively. Confining pressures, measured by means of a manganin coil exposed directly to the pressure medium, are accurate to within 1%. The reported densities are bulk densities calculated from the weights and dimensions of the cylindrical samples.

Pressure Induced Crack Closure

To be useful in the interpretation of crustal seismic investigations laboratory measured velocities need to be obtained at appropriate elevated confining pressures. At atmospheric pressure most igneous and metamorphic rocks contain cracks characterized by very low aspect-ratios (minimum/maximum dimensions). These cracks are usually attributed to cooling and decompression accompanying their uplift to the Earths surface [e.g., *Birch*, 1960]. It has long been recognized that these cracks significantly lower velocities and many theoretical studies of the elasticity of cracked solids have focused on the influence of low aspect-ratio cracks on velocities and their changes with applied stress [e.g., *O'Connell and Budiansky*, 1974].

As expected the measured wave velocities in Table 2 are low and extremely pressure sensitive for pressures below approximately 100 to 200 MPa. At higher pressures the grain boundary cracks are closed and the velocities are related to the elastic properties of the constituent minerals of the rocks. Thus most interpretations of field measured velocities at significant crustal depths require laboratory measurements at elevated confining pressures. Likewise correlations of rock velocities with mineralogy require measurements at pressures above those of crack closure.

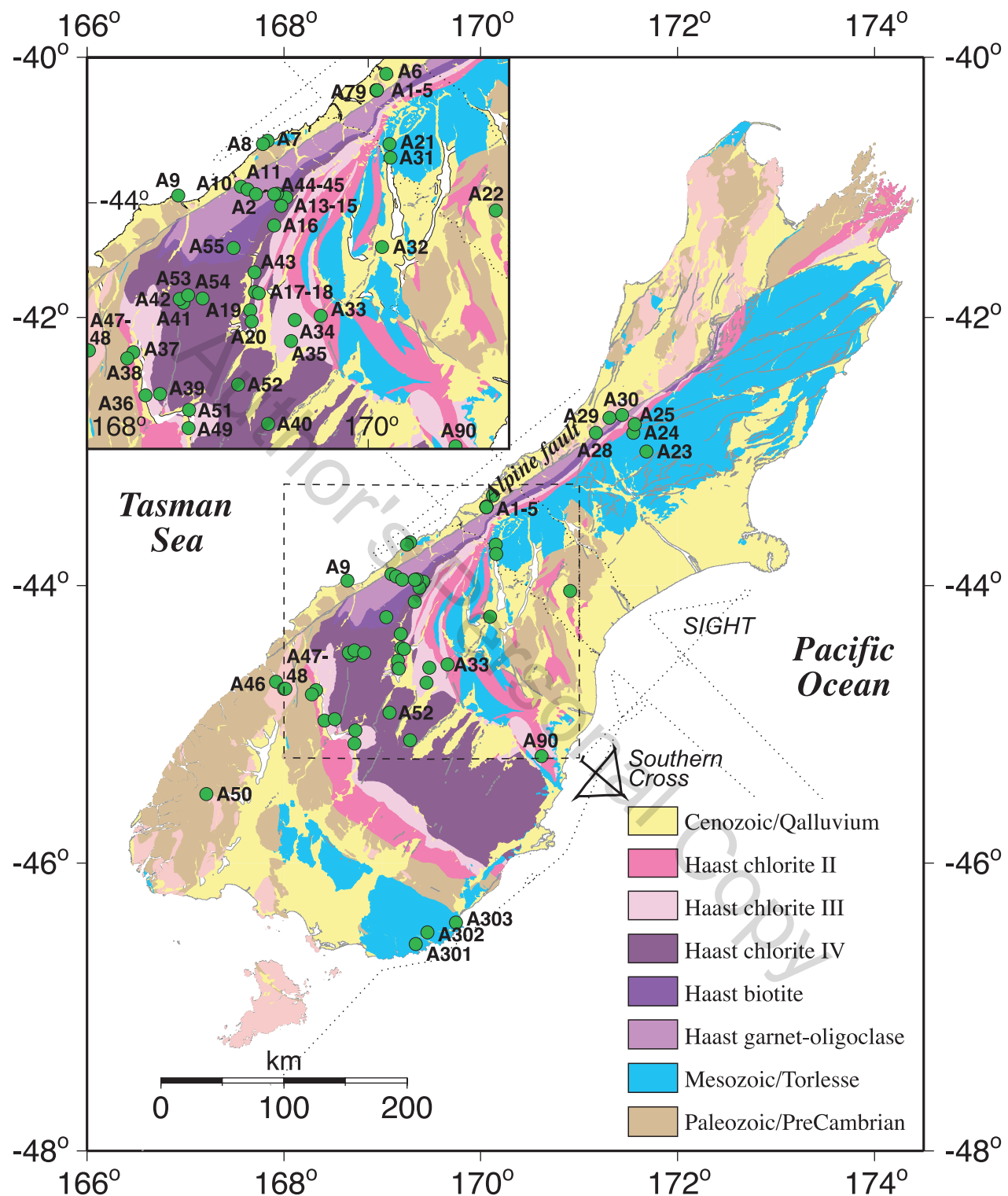


Plate 1. Terrane map of South Island showing locations of rocks collected for velocity measurements. Circles denote sample locations; inset map provides names of samples within dashed box. See Tables 1–3 for sample information. Dotted lines denote SIGHT marine ship tracks. Location of Southern Cross experiment shown (for Plate 2).

Table 1. Rock samples used in this study. Locations shown in Plate 1. Digital version of this table is on the CDROM which accompanies this volume.

Sample	Rock	Zone	Terrane	density (kg/m ³)	Longitude (E)	Latitude (S)	Location
A-1	Garnet schist	garnet zone	Alpine Schist	2723	170°03'31"	43°25'03"	Fox Glacier
A-2	Mica schist	garnet zone	Alpine Schist	2765	170°03'31"	43°25'06"	Fox Glacier
A-3	Garnet schist	garnet zone	Alpine Schist	2735	170°03'33"	43°25'06"	Fox Glacier
A-4	Garnet schist	garnet zone	Alpine Schist	2668	170°03'40"	43°25'10"	Fox Glacier
A-5	Garnet schist	garnet zone	Alpine Schist	2656	170°03'40"	43°25'10"	Fox Glacier
A-6	Phyllite		Greenland Group	2713	170°07'42"	43°20'00"	Omoeroa R.
A-7	Phyllite		Greenland Group	2640	169°17'10"	43°40'45"	Lake Moeraki
A-8	Phyllite		Greenland Group	2642	169°15'00"	43°41'50"	Whakapohai R.
A-9	Phyllite		Greenland Group	2644	168°39'00"	43°57'45"	Jackson Bay
A-10	Schist	garnet zone	Alpine Schist	2700	169°05'40"	43°54'58"	Big Bluff
A-11	Schist	garnet zone	Alpine Schist	2694	169°08'30"	43°55'53"	Thomas Bluff
A-12	Schist	garnet zone	Alpine Schist	2713	169°12'10"	43°57'20"	Halfway Bluff
A-13	Schist	biotite zone	Alpine Schist	2712	169°22'00"	43°57'40"	Evans Creek
A-14	Greenschist	chlorite zone IV	Alpine Schist	2681	169°25'07"	43°58'15"	Clarke Bluff
A-15	Greenschist	chlorite zone IV	Alpine Schist	2656	169°22'53"	44°00'48"	Mather Creek
A-16	Greenschist	chlorite zone IV	Alpine Schist	2714	169°19'55"	44°06'55"	Fish R.
A-17	Greenschist	chlorite zone IV	Otago Schist	3002	169°11'40"	44°27'15"	Lake Hawea
A-18	Greenschist	chlorite zone III	Otago Schist	2726	169°13'15"	44°27'45"	Lake Hawea
A-19	Greenschist	chlorite zone II	Otago Schist	2735	169°09'45"	44°32'50"	Lake Hawea
A-20	Greenschist (Greywacke)	chlorite zone II	Otago Schist	2708	169°10'20"	44°36'20"	Lake Hawea
A-21	Torlesse greywacke		Rakaia Terrane	2737	170°09'10"	43°41'50"	Wakefield Falls
A-22	Torlesse greywacke		Rakaia Terrane	2690	170°54'35"	44°02'20"	Allandale
A-23	Torlesse greywacke		Rakaia Terrane	2688	171°41'10"	43°00'20"	Corner Knob
A-24	Torlesse greywacke		Rakaia Terrane	2654	171°33'06"	42°52'08"	Windy Pt
A-25	Torlesse greywacke		Rakaia Terrane	2706	171°34'04"	42°48'11"	Kellys Creek
A-26	Jadestone		Alpine Schist	2971			Hokitika
A-28	Tuhua Granite		Tuhua Granite	2631	171°10'15"	42°52'00"	Mt Tuhua
A-29	Tuhua Granite		Tuhua Granite	2650	171°18'41"	42°45'25"	Fitzgerald Ck
A-30	Alpine fault mylonite		Alpine Schist	2677	171°26'18"	42°44'00"	Rocky Pt
A-3 IB	Torlesse greywacke		Rakaia Terrane	2705	170°09'40"	43°46'00"	Lake Pukaki
A-32B	Torlesse greywacke		Rakaia Terrane	2756	170°06'00"	44°13'30"	Twizel Power House
A-33	Greenschist	chlorite zone II	Otago Schist	2624	169°39'50"	44°34'30"	Lindis Pass
A-34	Greenschist	chlorite zone III	Otago Schist	2701	169°28'40"	44°35'48"	Dip Creek

Table 1. (Continued)

Sample	Rock	Zone	Terrane	density (kg/m ³)	Longitude (E)	Latitude (S)	Location
A-35	Greenschist	chlorite zone III	Otago Schist	2741	169°27'00"	44°42'20"	N Lindis Valley
A-36	Greenschist	chlorite zone III	Otago Schist	2783	169°25'00"	44°58'45"	White Pt
A-37	Greenschist	chlorite zone III	Otago Schist	2742	169°19'50"	44°45'40"	Glenorchy
A-38	Greenschist (Greywacke)	chlorite zone II	Otago Schist	2749	168°17'10"	44°47'30"	S Kinloch
A-39	Greenschist	chlorite zone II	Otago Schist	2762	168°31'10"	44°58'18"	Lake Dispute
A-40	Biotite schist	chlorite zone IV	Otago Schist	2649	169°17'12"	45°07'21"	Waikeriker
A-41	Epidote amphibolite		Otago Schist	2955	168°41'07"	44°30'30"	Brides Veil Str
A-42	Greenschist	chlorite zone IV	Otago Schist	2659	168°39'37"	44°29'25"	Aspiring Cascade Huts
A-43	Greenschist	chlorite zone IV	Otago Schist	2746	169°11'30"	44°21'15"	Lake Wanaka
A-44	Biotite schist	biotite zone	Otago Schist	2715	169°21'08"	43°57'10"	Douglas Bluff
A-45	Biotite schist	biotite zone	Otago Schist	2700	169°19'50"	43°57'20"	Douglas Crk
A-46	Hornblende gabbro		Darran	2896	167°55'15"	44°42'01"	Homer Tunnel
A-47	Hornblende gabbro		Mackay Intrusives	3032	168°00'00"	44°45'00"	Hollylord R
A-48	Gabbro		Mackay Intrusives	2857	168°00'50"	44°45'05"	Falls Creek
A-49	Greenschist	chlorite zone IV	Otago Schist	2768	168°43'15"	45°08'40"	Devils Staircase
A-50	Felsic gneiss			2679	167°12'45"	45°30'27"	Pahiri Peak
A-51	Greenschist	chlorite zone III	Otago Schist	2732	168°43'35"	45°03'10"	Wye Creek
A-52	Epidote amphibolite		Otago Schist	2968	169°04'35"	44°55'25"	Kawarau Gorge
A-53	Epidote amphibolite		Otago Schist	3030	168°43'10"	44°28'16"	Rob Roy Str
A-54	Amphibolite		Otago Schist	2819	168°49'17"	44°29'17"	Glenlinnan Str
A-55	Biotite schist	biotite zone	Otago Schist	2641	169°02'30"	44°13'52"	Kerin Forks
A-79	Garnet amphibolite		Alpine Schist	2911	170°03'42"	43°25'10"	Fox Glacier
A-90	Greenschist	chlorite zone II	Otago Schist	2512	170°37'20"	46°14'12"	
A-301	Greywacke		Murihiku	2710	169°45'00"	46°34'10"	
A-302	Greywacke		Murihiku	2509	169°27'35"	46°29'15"	
A-303	Argillite		Murihiku	2596	169°20'30"	46°25'10"	

Table 2. Velocity measurements

#	core	Pressure (MPa)										
		20	40	60	80	100	200	400	600	800	1000	
A-1	Vp	A	3.855	4.430	4.783	5.011	5.163	5.472	5.651	5.750	5.823	5.879
	Vp	B	5.419	5.661	5.826	5.947	6.038	6.268	6.405	6.468	6.511	6.545
	Vp	C	5.499	5.769	5.642	6.060	6.143	6.339	6.466	6.534	6.583	6.621
	Vp	mean	4.924	5.287	5.417	5.672	5.781	6.026	6.174	6.251	6.306	6.349
	Vs	A	2.608	2.843	2.997	3.103	3.177	3.338	3.418	3.457	3.484	3.506
	Vs	B	3.372	3.524	3.627	3.699	3.750	3.862	3.911	3.931	3.944	3.955
	Vs	C	2.623	2.800	2.903	3.101	3.009	3.101	3.168	3.207	3.235	3.257
	Vs	mean	2.868	3.055	3.175	3.301	3.312	3.434	3.499	3.531	3.554	3.572
	Vp/Vs	mean	1.717	1.730	1.706	1.719	1.746	1.755	1.765	1.770	1.774	1.777
	σ	mean	0.243	0.249	0.238	0.244	0.256	0.260	0.263	0.266	0.267	0.268
A-2	Vp	A	3.790	4.377	4.721	4.930	5.063	5.312	5.458	5.541	5.600	5.648
	Vp	B	4.997	5.443	5.718	5.895	6.011	6.239	6.354	6.415	6.459	6.493
	Vp	C	4.559	5.088	5.433	5.667	5.828	6.156	6.300	6.366	6.744	6.451
	Vp	mean	4.449	4.969	5.291	5.497	5.634	5.902	6.037	6.107	6.268	6.197
	Vs	A	2.608	2.784	2.882	2.911	2.980	3.071	3.148	3.194	3.228	3.254
	Vs	B	3.155	3.464	3.657	3.780	3.856	4.002	4.054	4.078	4.096	4.109
	Vs	C	2.607	2.862	3.006	3.105	3.169	3.288	3.334	3.357	3.373	3.385
	Vs	mean	2.790	3.037	3.182	3.265	3.335	3.453	3.512	3.543	3.565	3.583
	Vp/Vs	mean	1.595	1.636	1.663	1.684	1.689	1.709	1.719	1.724	1.758	1.730
	σ	mean	0.176	0.202	0.217	0.227	0.230	0.240	0.244	0.246	0.261	0.249
A-3	Vp	A	4.409	4.738	4.949	5.094	5.199	5.449	5.622	5.717	5.785	5.839
	Vp	B	5.216	5.533	5.735	5.873	5.971	6.197	6.341	6.418	6.474	6.517
	Vp	C	5.427	5.674	5.836	5.952	6.038	6.256	6.404	6.481	6.563	6.579
	Vp	mean	5.017	5.315	5.507	5.640	5.736	5.967	6.122	6.205	6.274	6.312
	Vs	A	2.889	3.023	3.114	3.179	3.228	3.351	3.424	3.459	3.483	3.503
	Vs	B	3.324	3.457	3.550	3.617	3.666	3.778	3.824	3.841	3.852	3.860
	Vs	C	2.517	2.776	2.935	3.036	3.102	3.226	3.286	3.318	3.341	3.359
	Vs	mean	2.910	3.086	3.200	3.277	3.332	3.451	3.512	3.539	3.559	3.574
	Vp/Vs	mean	1.724	1.723	1.721	1.721	1.721	1.729	1.743	1.753	1.763	1.766
	σ	mean	0.247	0.246	0.245	0.245	0.245	0.249	0.255	0.259	0.263	0.264
A-4	Vp	A	3.551	4.311	4.810	5.147	5.377	5.838	6.025	6.110	6.172	6.220
	Vp	B	4.480	4.966	5.301	5.539	5.711	6.089	6.245	6.304	6.344	6.376
	Vp	C	4.133	4.756	5.173	5.460	5.661	6.072	6.232	6.297	6.344	6.380
	Vp	mean	4.054	4.677	5.095	5.382	5.583	6.000	6.168	6.237	6.286	6.325
	Vs	A	2.412	2.801	3.058	3.233	3.353	3.587	3.666	3.697	3.719	3.735
	Vs	B	2.692	3.018	3.239	3.390	3.494	3.693	3.744	3.757	3.765	3.772
	Vs	C	2.353	2.748	3.004	3.172	3.285	3.490	3.552	3.578	3.596	3.609
	Vs	mean	2.486	2.856	3.100	3.265	3.377	3.590	3.654	3.677	3.693	3.706
	Vp/Vs	mean	1.631	1.638	1.643	1.648	1.653	1.671	1.688	1.696	1.702	1.707
	σ	mean	0.199	0.203	0.206	0.209	0.211	0.221	0.230	0.234	0.236	0.239

Table 2. (Continued)

#	core	Pressure (MPa)										
		20	40	60	80	100	200	400	600	800	1000	
A-5	Vp	A	4.104	4.433	4.643	4.793	4.905	5.207	5.454	5.596	5.699	5.780
	Vp	B	5.382	5.600	5.740	5.835	5.901	6.045	6.123	6.163	6.191	6.213
	Vp	C	5.665	5.979	6.148	6.243	6.300	6.041	6.476	6.517	6.546	6.569
	Vp	mean	5.050	5.337	5.510	5.624	5.702	5.764	6.018	6.092	6.145	6.188
	Vs	A	2.708	2.866	2.977	3.061	3.127	3.303	3.409	3.452	3.481	3.503
	Vs	B	3.027	3.187	3.303	3.390	3.457	3.620	3.691	3.710	3.722	3.731
	Vs	C	1.974	2.125	2.232	2.317	2.385	2.840	2.752	2.817	2.859	2.890
	Vs	mean	2.569	2.726	2.837	2.923	2.990	3.254	3.284	3.326	3.354	3.375
	Vp/Vs	mean	1.965	1.958	1.942	1.924	1.907	1.771	1.832	1.831	1.832	1.833
	σ	mean	0.325	0.324	0.320	0.315	0.310	0.266	0.288	0.288	0.288	0.288
A-6	Vp	A	5.657	5.776	5.847	5.894	5.927	6.017	6.097	6.143	6.177	6.203
	Vp	B	5.440	5.581	5.668	5.729	5.773	5.893	5.994	6.052	6.093	6.125
	Vp	C	5.323	5.476	5.558	5.609	5.645	5.742	5.834	5.889	5.929	5.959
	Vp	mean	5.473	5.611	5.691	5.744	5.782	5.884	5.975	6.028	6.066	6.096
	Vs	A	3.668	3.734	3.776	3.805	3.826	3.877	3.914	3.935	3.949	3.960
	Vs	B	3.345	3.409	3.453	3.484	3.507	3.563	3.593	3.607	3.617	3.624
	Vs	C	3.448	3.498	3.533	3.559	3.578	3.628	3.657	3.668	3.676	3.682
	Vs	mean	3.487	3.547	3.587	3.616	3.637	3.689	3.721	3.737	3.747	3.755
	Vp/Vs	mean	1.570	1.582	1.586	1.588	1.590	1.595	1.606	1.613	1.619	1.623
	σ	mean	0.158	0.167	0.170	0.172	0.173	0.176	0.183	0.188	0.191	0.194
A-7	Vp	A	3.622	4.167	4.496	4.706	4.847	5.150	5.359	5.481	5.570	5.641
	Vp	B	5.784	5.903	5.983	6.042	6.088	6.213	6.299	6.339	6.367	6.389
	Vp	C	5.387	5.558	5.668	5.747	5.807	5.967	6.088	6.153	6.199	6.235
	Vp	mean	4.931	5.209	5.382	5.499	5.581	5.777	5.915	5.991	6.046	6.088
	Vs	A	2.837	2.968	3.054	3.118	3.168	3.311	3.421	3.478	3.517	3.548
	Vs	B	3.628	3.690	3.732	3.762	3.786	3.845	3.881	3.897	3.908	3.917
	Vs	C	2.817	2.935	3.015	3.074	3.120	3.247	3.332	3.372	3.400	3.421
	Vs	mean	3.094	3.197	3.267	3.318	3.358	3.467	3.545	3.582	3.608	3.629
	Vp/Vs	mean	1.594	1.629	1.648	1.657	1.662	1.666	1.669	1.672	1.675	1.678
	σ	mean	0.175	0.198	0.208	0.214	0.216	0.218	0.220	0.222	0.223	0.224
A-8	Vp	A	3.070	3.350	3.560	6.729	3.871	4.327	4.686	4.819	4.891	4.942
	Vp	B	5.929	6.044	6.129	6.196	6.249	6.396	6.479	6.505	6.519	6.530
	Vp	C	6.227	6.351	6.430	6.484	6.522	6.607	6.658	6.685	6.704	6.718
	Vp	mean	5.075	5.248	5.373	6.470	5.547	5.777	5.941	6.003	6.038	6.064
	Vs	A	1.945	2.079	2.167	2.235	2.289	2.470	2.651	2.748	2.814	2.864
	Vs	B	3.083	3.198	3.278	3.341	3.392	3.560	3.706	3.770	3.809	3.838
	Vs	C	1.755	1.896	1.993	2.068	2.130	2.336	2.534	2.632	2.694	2.741
	Vs	mean	2.261	2.391	2.479	2.548	2.604	2.789	2.964	3.050	3.106	3.148
	Vp/Vs	mean	2.245	2.195	2.167	2.539	2.130	2.071	2.005	1.968	1.944	1.926
	σ	mean	0.376	0.369	0.365	0.408	0.359	0.348	0.334	0.326	0.320	0.316

Table 2. (Continued)

#	core	Pressure (MPa)										
		20	40	60	80	100	200	400	600	800	1000	
A-9	Vp	A	4.296	4.758	5.042	5.224	5.345	5.586	5.666	5.788	5.839	5.879
	Vp	B	4.772	5.064	5.259	5.396	5.495	5.724	5.849	5.909	5.952	5.985
	Vp	C	5.271	5.539	5.697	5.796	5.861	5.993	6.079	6.127	6.162	6.189
	Vp	mean	4.780	5.120	5.333	5.472	5.567	5.768	5.865	5.941	5.984	6.017
	Vs	A	2.959	3.161	3.281	3.356	3.406	3.507	3.571	3.608	3.634	3.655
	Vs	B	3.198	3.334	3.425	3.488	3.533	3.633	3.681	3.703	3.718	3.730
	Vs	C	3.122	3.210	3.269	3.312	3.344	3.420	3.459	3.476	3.487	3.496
	Vs	mean	3.093	3.235	3.325	3.385	3.428	3.520	3.570	3.596	3.613	3.627
	Vp/Vs	mean	1.545	1.583	1.604	1.616	1.624	1.639	1.643	1.652	1.656	1.659
	σ	mean	0.140	0.168	0.182	0.190	0.195	0.203	0.206	0.211	0.213	0.215
A-10	Vp	A	3.999	4.416	4.707	4.922	5.087	5.511	5.763	5.874	5.952	6.014
	Vp	B	4.284	4.757	5.073	5.294	5.452	5.810	5.998	6.088	6.152	6.203
	Vp	C	4.620	5.124	5.448	5.668	5.820	6.146	6.319	6.408	6.472	6.522
	Vp	mean	4.301	4.766	5.076	5.295	5.453	5.822	6.027	6.123	6.192	6.246
	Vs	A	2.472	2.730	2.907	3.034	3.126	3.338	3.440	3.483	3.513	3.536
	Vs	B	2.880	3.127	3.288	3.398	3.474	3.640	3.724	3.765	3.794	3.817
	Vs	C	2.378	2.634	2.807	2.930	3.018	3.218	3.314	3.356	3.387	3.410
	Vs	mean	2.577	2.830	3.001	3.120	3.206	3.399	3.493	3.535	3.565	3.588
	Vp/Vs	mean	1.669	1.684	1.692	1.697	1.701	1.713	1.726	1.732	1.737	1.741
	σ	mean	0.220	0.228	0.231	0.234	0.236	0.242	0.247	0.250	0.252	0.254
A-11	Vp	A	2.841	3.708	4.281	4.670	4.939	5.486	5.723	5.836	5.918	5.984
	Vp	B	4.887	5.347	5.656	5.871	6.024	6.351	6.494	6.554	6.597	6.631
	Vp	C	4.328	4.885	5.270	5.521	5.707	6.105	6.279	6.353	6.406	6.447
	Vp	mean	4.019	4.646	5.069	5.354	5.556	5.981	6.165	6.248	6.307	6.354
	Vs	A	2.203	2.559	2.787	2.938	3.039	3.237	3.322	3.364	3.393	3.416
	Vs	B	3.059	3.298	3.455	3.561	3.634	3.785	3.850	3.880	3.901	3.917
	Vs	C	2.202	2.548	2.768	2.913	3.010	3.197	3.278	3.318	3.347	3.370
	Vs	mean	2.488	2.802	3.003	3.137	3.228	3.406	3.483	3.521	3.547	3.568
	Vp/Vs	mean	1.615	1.659	1.688	1.707	1.721	1.756	1.770	1.775	1.778	1.781
	σ	mean	0.189	0.214	0.230	0.239	0.245	0.260	0.266	0.267	0.269	0.270
A-12	Vp	A	3.324	4.044	4.518	4.841	5.066	5.536	5.757	5.865	5.943	6.005
	Vp	B	4.008	4.624	5.040	5.330	5.537	5.986	6.192	6.283	6.348	6.399
	Vp	C	4.704	5.189	5.521	5.756	5.926	6.303	6.469	6.537	6.584	6.621
	Vp	mean	4.012	4.619	5.026	5.309	5.509	5.942	6.140	6.228	6.292	6.342
	Vs	A	2.271	2.588	2.804	2.955	3.062	3.289	3.379	3.415	3.440	3.460
	Vs	B	2.768	3.039	3.228	3.366	3.469	3.715	3.834	3.881	3.913	3.938
	Vs	C	1.870	2.287	2.545	2.709	2.815	3.002	3.074	3.109	3.134	3.154
	Vs	mean	2.303	2.638	2.859	3.010	3.115	3.335	3.429	3.468	3.496	3.517
	Vp/Vs	mean	1.742	1.751	1.758	1.764	1.768	1.781	1.790	1.796	1.800	1.803
	σ	mean	0.254	0.258	0.261	0.263	0.265	0.270	0.273	0.275	0.277	0.278

Table 2. (Continued)

#	core	Pressure (MPa)										
		20	40	60	80	100	200	400	600	800	1000	
A-13	Vp	A	2.931	3.840	4.431	4.825	5.090	5.596	5.784	5.869	5.931	5.980
	Vp	B	5.496	6.802	6.368	6.571	6.700	6.918	6.997	7.035	7.063	7.084
	Vp	C	4.786	5.258	5.583	5.815	5.983	6.355	6.512	6.572	6.614	6.646
	Vp	mean	4.404	5.300	5.461	5.737	5.924	6.289	6.431	6.492	6.536	6.570
	Vs	A	2.280	2.624	2.840	2.980	3.073	3.253	3.337	3.380	3.411	3.436
	Vs	B	2.848	3.254	3.499	3.650	3.746	3.909	3.972	4.005	4.028	4.046
	Vs	C	2.112	2.524	2.789	2.962	3.077	3.286	3.353	3.382	3.402	3.417
	Vs	mean	2.414	2.801	3.043	3.198	3.299	3.482	3.554	3.589	3.614	3.633
	Vp/Vs	mean	1.825	1.892	1.795	1.794	1.796	1.806	1.809	1.809	1.809	1.809
	σ	mean	0.285	0.306	0.275	0.275	0.275	0.279	0.280	0.280	0.280	0.280
A-14	Vp	A	2.771	3.666	4.279	4.709	5.013	5.656	5.910	6.012	6.085	6.144
	Vp	B	3.549	4.298	4.806	5.161	5.412	5.940	6.151	6.237	6.298	6.375
	Vp	C	4.176	4.785	5.204	5.500	5.712	6.174	6.361	6.433	6.483	6.522
	Vp	mean	3.499	4.250	4.763	5.123	5.379	5.923	6.141	6.227	6.288	6.347
	Vs	A	2.174	2.653	2.959	3.158	3.290	3.528	3.607	3.642	3.666	3.685
	Vs	B	2.577	2.944	3.180	3.336	3.441	3.638	3.710	3.743	3.766	3.783
	Vs	C	1.918	2.482	2.844	3.082	3.239	3.526	3.621	3.663	3.693	3.716
	Vs	mean	2.223	2.693	2.994	3.192	3.323	3.564	3.646	3.682	3.708	3.728
	Vp/Vs	mean	1.574	1.578	1.591	1.605	1.619	1.662	1.684	1.691	1.696	1.702
	σ	mean	0.161	0.165	0.173	0.183	0.191	0.216	0.228	0.231	0.233	0.237
A-15	Vp	A	2.904	3.577	4.066	4.439	4.728	5.495	5.936	6.112	6.233	6.329
	Vp	B	4.963	5.222	5.401	5.538	5.646	5.963	6.193	6.294	6.362	6.414
	Vp	C	4.309	4.836	5.204	5.474	5.675	6.163	6.411	6.513	6.584	6.639
	Vp	mean	4.059	4.545	4.891	5.150	5.350	5.874	6.180	6.306	6.393	6.461
	Vs	A	2.053	2.420	2.674	2.857	2.993	3.314	3.480	3.554	3.606	3.647
	Vs	B	3.062	3.224	3.341	3.430	3.499	3.685	3.791	3.829	3.845	3.874
	Vs	C	1.932	2.345	2.624	2.821	2.961	3.268	3.410	3.474	3.520	3.557
	Vs	mean	2.349	2.663	2.880	3.036	3.151	3.422	3.560	3.619	3.657	3.693
	Vp/Vs	mean	1.728	1.707	1.698	1.696	1.698	1.716	1.736	1.743	1.748	1.750
	σ	mean	0.248	0.239	0.235	0.234	0.234	0.243	0.252	0.254	0.257	0.257
A-16	Vp	A	2.939	3.541	3.961	4.270	4.504	5.102	5.474	5.656	5.787	5.892
	Vp	B	5.800	6.023	6.178	6.295	6.386	6.632	6.786	6.850	6.893	6.927
	Vp	C	5.441	5.755	5.962	6.107	6.212	6.453	6.588	6.654	6.701	6.737
	Vp	mean	4.727	5.106	5.367	5.557	5.700	6.062	6.283	6.386	6.460	6.519
	Vs	A	2.195	2.425	2.580	2.691	2.773	2.976	3.101	3.164	3.208	3.244
	Vs	B	3.523	3.674	3.778	3.851	3.903	4.014	4.054	4.068	4.078	4.085
	Vs	C	2.364	2.581	2.727	2.819	2.903	3.068	3.147	3.182	3.207	3.223
	Vs	mean	2.694	2.893	3.028	3.120	3.193	3.353	3.434	3.471	3.498	3.517
	Vp/Vs	mean	1.755	1.765	1.772	1.781	1.785	1.808	1.829	1.840	1.847	1.853
	σ	mean	0.259	0.264	0.267	0.270	0.271	0.280	0.287	0.290	0.293	0.295

Table 2. (Continued)

#	core	Pressure (MPa)										
		20	40	60	80	100	200	400	600	800	1000	
A-17	Vp	A	3.309	4.588	5.052	5.335	5.513	5.828	5.983	6.069	6.131	6.180
	Vp	B	5.000	5.402	5.673	5.864	6.003	6.316	6.471	6.541	6.590	6.629
	Vp	C	5.517	5.799	5.987	6.121	6.220	6.457	6.593	6.657	6.702	6.738
	Vp	mean	4.609	5.263	5.571	5.774	5.912	6.200	6.349	6.422	6.474	6.515
	Vs	A	2.747	2.973	3.115	3.209	3.271	3.392	3.446	3.472	3.491	3.506
	Vs	B	3.292	2.463	3.575	3.622	3.705	3.815	3.862	3.883	3.898	3.909
	Vs	C	2.551	2.793	2.950	3.056	3.130	3.286	3.366	3.407	3.436	3.458
	Vs	mean	2.863	2.743	3.214	3.296	3.369	3.498	3.558	3.587	3.608	3.624
	Vp/Vs	mean	1.610	1.919	1.734	1.752	1.755	1.772	1.784	1.790	1.794	1.798
	σ	mean	0.186	0.314	0.251	0.258	0.260	0.267	0.271	0.273	0.275	0.276
A-18	Vp	A	3.643	4.053	4.344	4.569	4.749	5.283	5.675	5.850	5.967	6.059
	Vp	B	5.430	5.674	5.846	5.980	6.087	6.408	6.640	6.733	6.793	6.838
	Vp	C	5.202	5.449	5.319	5.749	5.854	6.163	6.395	6.498	6.566	6.619
	Vp	mean	4.758	5.059	5.170	5.433	5.563	5.952	6.237	6.360	6.442	6.505
	Vs	A	2.939	2.587	2.716	2.814	2.892	3.113	3.274	3.350	3.403	3.444
	Vs	B	3.317	3.434	3.520	3.587	3.640	3.787	3.872	3.900	3.918	3.931
	Vs	C	2.351	2.530	2.659	2.759	2.839	3.078	3.246	3.314	3.358	3.391
	Vs	mean	2.869	2.850	2.965	3.053	3.124	3.326	3.464	3.522	3.559	3.589
	Vp/Vs	mean	1.659	1.775	1.744	1.779	1.781	1.789	1.800	1.806	1.810	1.813
	σ	mean	0.214	0.267	0.255	0.269	0.270	0.273	0.277	0.279	0.280	0.281
A-19	Vp	A	4.250	4.722	5.038	5.261	5.423	5.801	6.014	6.119	6.194	6.253
	Vp	B	5.802	6.026	6.169	6.267	6.337	6.500	6.607	6.664	6.704	6.736
	Vp	C	4.950	5.274	5.487	5.638	5.751	6.034	6.227	6.329	6.401	6.458
	Vp	mean	5.001	5.341	5.565	5.722	5.837	6.112	6.283	6.370	6.433	6.482
	Vs	A	2.979	3.152	3.265	3.342	3.397	3.520	3.589	3.624	3.650	3.669
	Vs	B	3.423	3.517	3.583	3.632	3.669	3.761	3.810	3.829	3.842	3.852
	Vs	C	3.191	3.300	3.363	3.400	3.423	3.462	3.482	3.492	3.500	3.505
	Vs	mean	3.198	3.323	3.404	3.458	3.496	3.581	3.627	3.648	3.664	3.675
	Vp/Vs	mean	1.564	1.607	1.635	1.655	1.669	1.707	1.732	1.746	1.756	1.764
	σ	mean	0.154	0.184	0.201	0.212	0.220	0.239	0.250	0.256	0.260	0.263
A-20	Vp	A	4.827	5.182	5.360	5.460	5.521	5.659	5.782	5.854	5.907	5.948
	Vp	B	6.302	6.425	6.495	6.539	6.569	6.643	6.708	6.745	6.772	6.793
	Vp	C	5.244	5.528	5.702	5.815	5.891	6.056	6.160	6.217	6.259	6.291
	Vp	mean	5.457	5.712	5.852	5.938	5.994	6.119	6.216	6.272	6.313	6.344
	Vs	A	3.237	3.298	3.338	3.368	3.391	3.460	3.514	3.541	3.559	3.574
	Vs	B	3.656	3.723	3.760	3.782	3.796	3.826	3.850	3.864	3.873	3.881
	Vs	C	3.493	3.529	3.550	3.566	3.577	3.609	3.635	3.650	3.660	3.669
	Vs	mean	3.462	3.517	3.549	3.572	3.588	3.632	3.666	3.685	3.697	3.708
	Vp/Vs	mean	1.576	1.624	1.649	1.662	1.670	1.685	1.696	1.702	1.707	1.711
	σ	mean	0.163	0.195	0.209	0.216	0.221	0.228	0.233	0.236	0.239	0.241

Table 2. (Continued)

#	core	Pressure (MPa)										
		20	40	60	80	100	200	400	600	800	1000	
A-21	Vp	A	5.874	6.000	6.068	6.111	6.140	6.214	6.284	6.324	6.353	6.376
	Vp	B	5.859	5.952	6.007	6.045	6.073	6.152	6.225	6.268	6.298	6.322
	Vp	C	5.890	5.991	6.049	6.087	6.115	6.189	6.259	6.300	6.329	6.352
	Vp	mean	5.874	5.981	6.041	6.081	6.109	6.185	6.256	6.297	6.327	6.350
	Vs	A	3.542	3.576	3.597	3.612	3.623	3.654	3.680	3.695	3.706	3.714
	Vs	B	3.541	3.573	3.593	3.607	3.619	3.650	3.676	3.689	3.699	3.706
	Vs	C	3.548	3.580	3.602	3.617	3.629	3.660	3.684	3.697	3.705	3.712
	Vs	mean	3.544	3.576	3.597	3.612	3.623	3.655	3.680	3.694	3.703	3.711
	Vp/Vs	mean	1.658	1.672	1.680	1.684	1.686	1.692	1.700	1.705	1.708	1.711
	σ	mean	0.214	0.222	0.225	0.227	0.229	0.232	0.235	0.238	0.239	0.241
A-22	Vp	A	5.838	5.895	5.925	5.945	5.961	6.013	6.078	6.122	6.154	6.179
	Vp	B	5.913	5.969	6.001	6.024	6.042	6.099	6.161	6.199	6.226	6.247
	Vp	C	5.978	6.032	6.063	6.085	6.102	6.158	6.216	6.250	6.275	6.294
	Vp	mean	5.910	5.965	5.996	6.018	6.035	6.090	6.152	6.190	6.218	6.240
	Vs	A	3.551	3.571	3.583	3.592	3.598	3.619	3.641	3.654	3.663	3.670
	Vs	B	3.507	3.539	3.558	3.570	3.580	3.604	3.625	3.637	3.646	3.653
	Vs	C	3.513	3.536	3.550	3.559	3.567	3.590	3.615	3.630	3.640	3.649
	Vs	mean	3.524	3.549	3.564	3.574	3.581	3.604	3.627	3.640	3.650	3.657
	Vp/Vs	mean	1.677	1.681	1.683	1.684	1.685	1.690	1.696	1.700	1.704	1.706
	σ	mean	0.224	0.226	0.227	0.228	0.228	0.230	0.234	0.236	0.237	0.238
A-23	Vp	A	5.430	5.291	5.826	5.902	5.948	6.045	6.125	6.172	6.205	6.232
	Vp	B	5.645	5.783	5.865	5.920	5.958	6.056	6.138	6.185	6.219	6.245
	Vp	C	5.443	5.640	5.758	5.835	5.887	6.011	6.106	6.160	6.198	6.228
	Vp	mean	5.506	5.571	5.816	5.885	5.931	6.038	6.123	6.172	6.208	6.235
	Vs	A	3.431	3.488	3.524	3.549	3.566	3.607	3.632	3.640	3.655	3.663
	Vs	B	2.386	3.425	3.452	3.472	3.488	3.534	3.564	3.576	3.584	3.590
	Vs	C	3.383	3.437	3.473	3.500	3.520	3.572	3.603	3.617	3.627	3.634
	Vs	mean	3.067	3.450	3.483	3.507	3.525	3.571	3.600	3.611	3.622	3.629
	Vp/Vs	mean	1.795	1.615	1.670	1.678	1.683	1.691	1.701	1.709	1.714	1.718
	σ	mean	0.275	0.189	0.220	0.225	0.227	0.231	0.236	0.240	0.242	0.244
A-24	Vp	A	5.275	5.528	5.696	5.813	5.896	6.086	6.187	6.235	6.269	6.295
	Vp	B	5.111	5.437	5.644	5.781	5.873	6.064	6.163	6.214	6.251	6.279
	Vp	C	5.168	5.428	5.604	5.731	5.823	6.043	6.160	6.213	6.250	6.278
	Vp	mean	5.184	5.465	5.648	5.775	5.864	6.064	6.170	6.221	6.256	6.284
	Vs	A	3.251	3.374	3.453	3.507	3.544	3.622	3.661	3.679	3.692	3.702
	Vs	B	3.192	3.316	3.399	3.456	3.497	3.585	3.623	3.640	3.651	3.660
	Vs	C	3.203	3.320	3.400	3.457	3.498	3.588	3.625	3.639	3.649	3.656
	Vs	mean	3.216	3.337	3.417	3.473	3.513	3.598	3.636	3.653	3.664	3.673
	Vp/Vs	mean	1.612	1.638	1.653	1.663	1.669	1.685	1.697	1.703	1.708	1.711
	σ	mean	0.187	0.203	0.211	0.217	0.220	0.228	0.234	0.237	0.239	0.241

Table 2. (Continued)

#	core	Pressure (MPa)										
		20	40	60	80	100	200	400	600	800	1000	
A-25	Vp	A	5.663	5.802	5.887	5.945	5.987	6.093	6.176	6.223	6.257	6.283
	Vp	B	5.475	5.690	5.816	5.895	5.947	6.067	6.159	6.212	6.250	6.279
	Vp	C	5.416	5.649	5.775	5.850	5.898	6.010	6.106	6.162	6.203	6.235
	Vp	mean	5.518	5.714	5.826	5.896	5.944	6.056	6.147	6.199	6.237	6.266
	Vs	A	3.415	3.476	3.516	3.543	3.562	3.608	3.637	3.652	3.663	3.671
	Vs	B	3.429	3.473	3.502	3.522	3.537	3.576	3.605	3.621	3.632	3.641
	Vs	C	3.339	3.379	3.403	3.422	3.429	3.485	3.532	3.556	3.573	3.585
	Vs	mean	3.395	3.443	3.474	3.495	3.509	3.556	3.591	3.610	3.623	3.632
	Vp/Vs	mean	1.626	1.660	1.677	1.687	1.694	1.703	1.712	1.717	1.722	1.725
	σ	mean	0.196	0.215	0.224	0.229	0.232	0.237	0.241	0.243	0.245	0.247
A-26	Vp	A	6.542	6.693	6.721	6.760	6.787	6.856	6.920	6.957	6.984	7.005
	Vp	B	7.087	7.205	7.268	7.305	7.328	7.378	7.419	7.442	7.459	7.472
	Vp	C	6.863	6.992	7.056	7.093	7.116	7.173	7.226	7.257	7.279	7.296
	Vp	mean	6.831	6.963	7.015	7.053	7.077	7.136	7.188	7.219	7.241	7.258
	Vs	A	3.881	3.920	3.944	3.959	3.970	3.996	4.012	4.021	4.028	4.033
	Vs	B	4.004	4.042	4.069	4.090	4.105	4.147	4.171	4.179	4.184	4.189
	Vs	C	3.923	3.960	3.981	3.996	4.008	4.051	4.102	4.133	4.155	4.172
	Vs	mean	3.936	3.974	3.998	4.015	4.028	4.065	4.095	4.111	4.122	4.131
	Vp/Vs	mean	1.735	1.752	1.755	1.756	1.757	1.756	1.755	1.756	1.756	1.757
	σ	mean	0.251	0.258	0.259	0.260	0.260	0.260	0.260	0.260	0.260	0.260
A-28	Vp	A	5.242	5.594	5.813	5.954	6.047	6.232	6.326	6.375	6.410	6.437
	Vp	B	5.018	5.443	5.712	5.888	6.006	6.235	6.338	6.389	6.426	6.454
	Vp	C	4.966	5.284	5.499	5.652	5.763	6.018	6.145	6.202	6.241	6.272
	Vp	mean	5.075	5.440	5.675	5.831	5.939	6.162	6.270	6.322	6.359	6.388
	Vs	A	3.083	3.282	3.408	3.489	3.542	3.636	3.666	3.678	3.687	3.694
	Vs	B	2.950	3.193	3.342	3.437	3.500	3.624	3.692	3.729	3.755	3.776
	Vs	C	2.892	3.124	3.278	3.382	3.452	3.585	3.622	3.635	3.644	3.650
	Vs	mean	2.975	3.200	3.343	3.436	3.498	3.615	3.660	3.681	3.695	3.707
	Vp/Vs	mean	1.706	1.700	1.698	1.697	1.698	1.704	1.713	1.718	1.721	1.723
	σ	mean	0.238	0.236	0.234	0.234	0.234	0.238	0.242	0.244	0.245	0.246
A-29	Vp	A	4.373	4.934	5.304	5.557	5.733	6.100	6.261	6.334	6.386	6.427
	Vp	B	4.440	5.062	5.450	5.699	5.864	6.175	6.315	6.387	6.439	6.479
	Vp	C	4.932	5.378	5.664	5.854	5.984	6.250	6.381	6.447	6.493	6.530
	Vp	mean	4.582	5.125	5.473	5.704	5.860	6.175	6.319	6.389	6.440	6.479
	Vs	A	2.650	3.036	3.276	3.427	3.524	3.686	3.732	3.751	3.764	3.775
	Vs	B	2.887	3.125	3.281	3.385	3.456	3.591	3.636	3.654	3.667	3.676
	Vs	C	2.853	3.127	3.309	3.432	3.517	3.685	3.746	3.771	3.788	3.802
	Vs	mean	2.797	3.096	3.289	3.415	3.499	3.654	3.705	3.725	3.740	3.751
	Vp/Vs	mean	1.638	1.655	1.664	1.670	1.675	1.690	1.706	1.715	1.722	1.727
	σ	mean	0.203	0.213	0.217	0.221	0.223	0.231	0.238	0.242	0.246	0.248

Table 2. (Continued)

#	core	Pressure (MPa)										
		20	40	60	80	100	200	400	600	800	1000	
A-30	Vp	A	4.595	5.023	5.303	5.492	5.621	5.883	5.992	6.041	6.076	6.103
	Vp	B	4.910	5.309	5.561	5.727	5.839	6.066	6.179	6.236	6.278	6.310
	Vp	C	5.358	5.624	5.803	5.929	6.020	6.225	6.325	6.369	6.401	6.425
	Vp	mean	4.954	5.319	5.556	5.716	5.827	6.058	6.165	6.216	6.251	6.279
	Vs	A	3.019	3.176	3.280	3.351	3.401	3.506	3.555	3.578	3.594	3.606
	Vs	B	3.303	3.451	3.546	3.610	3.652	3.735	3.766	3.780	3.789	3.797
	Vs	C	2.944	3.154	3.285	3.369	3.425	3.531	3.580	3.605	3.622	3.636
	Vs	mean	3.089	3.260	3.370	3.443	3.493	3.591	3.634	3.654	3.668	3.680
	Vp/Vs	mean	1.604	1.631	1.648	1.660	1.668	1.687	1.697	1.701	1.704	1.706
	σ	mean	0.182	0.199	0.209	0.215	0.220	0.229	0.234	0.236	0.237	0.238
A-31b	Vp	A	5.710	5.892	6.002	6.073	6.122	6.231	6.306	6.349	6.379	6.403
	Vp	B	5.669	5.829	5.929	5.996	6.044	6.160	6.241	6.286	6.318	6.343
	Vp	C	5.349	5.614	5.769	5.865	5.927	6.058	6.148	6.200	6.236	6.264
	Vp	mean	5.576	5.778	5.900	5.978	6.031	6.149	6.232	6.278	6.311	6.337
	Vs	A	3.490	3.554	3.596	3.625	3.646	3.696	3.727	3.742	3.752	3.761
	Vs	B	3.497	3.552	3.589	3.614	3.632	3.672	3.691	3.699	3.705	3.710
	Vs	C	3.398	3.456	3.493	3.519	3.537	3.582	3.610	3.625	3.635	3.643
	Vs	mean	3.462	3.521	3.559	3.586	3.605	3.650	3.676	3.689	3.698	3.705
	Vp/Vs	mean	1.611	1.641	1.658	1.667	1.673	1.685	1.695	1.702	1.707	1.711
	σ	mean	0.186	0.205	0.214	0.219	0.222	0.228	0.233	0.236	0.239	0.241
A-32b	Vp	A	5.327	5.465	5.556	5.627	5.684	5.877	6.064	6.156	6.213	6.254
	Vp	B	5.515	5.631	5.705	5.761	5.807	5.962	6.125	6.213	6.270	6.310
	Vp	C	5.519	5.641	5.720	5.781	5.831	5.997	6.164	6.248	6.301	6.338
	Vp	mean	5.454	5.579	5.661	5.723	5.774	5.946	6.118	6.206	6.261	6.301
	Vs	A	3.220	3.286	3.332	3.368	3.397	3.484	3.546	3.570	3.584	3.595
	Vs	B	3.383	3.444	3.483	3.511	3.532	3.587	3.627	3.648	3.663	3.675
	Vs	C	3.378	3.442	3.483	3.512	3.533	3.583	3.610	3.624	3.633	3.640
	Vs	mean	3.327	3.391	3.433	3.464	3.487	3.551	3.594	3.614	3.627	3.637
	Vp/Vs	mean	1.639	1.645	1.649	1.652	1.656	1.674	1.702	1.717	1.726	1.732
	σ	mean	0.204	0.207	0.209	0.211	0.213	0.223	0.236	0.243	0.248	0.250
A-33	Vp	A	3.404	3.900	4.237	4.500	4.711	5.330	5.768	5.954	6.079	6.176
	Vp	B	4.251	4.623	4.892	5.102	5.271	5.760	6.084	6.207	6.286	6.345
	Vp	C	4.578	4.988	5.267	5.470	5.622	5.996	6.213	6.313	6.384	6.439
	Vp	mean	4.078	4.504	4.799	5.024	5.201	5.695	6.022	6.158	6.249	6.320
	Vs	A	2.100	2.439	2.566	2.845	2.974	3.292	3.475	3.559	3.620	3.664
	Vs	B	2.699	2.980	3.172	3.310	3.412	3.656	3.788	3.848	3.890	3.923
	Vs	C	2.615	2.805	2.937	3.035	3.110	3.309	3.430	3.482	3.519	3.547
	Vs	mean	2.471	2.741	2.892	3.063	3.165	3.419	3.564	3.630	3.676	3.711
	Vp/Vs	mean	1.650	1.643	1.660	1.640	1.643	1.666	1.690	1.697	1.700	1.703
	σ	mean	0.210	0.206	0.215	0.204	0.206	0.218	0.230	0.234	0.235	0.237

Table 2. (Continued)

#	core	Pressure (MPa)										
		20	40	60	80	100	200	400	600	800	1000	
A-34	Vp	A	4.049	4.483	4.763	4.955	5.093	5.419	5.636	5.756	5.843	5.911
	Vp	B	5.682	5.939	6.109	6.229	6.316	6.524	6.647	6.707	6.750	6.783
	Vp	C	4.625	5.012	5.268	5.448	5.578	5.881	6.056	6.143	6.206	6.255
	Vp	mean	4.786	5.145	5.380	5.544	5.662	5.941	6.113	6.202	6.266	6.316
	Vs	A	2.747	2.921	3.034	3.114	3.171	3.306	3.387	3.428	3.457	3.480
	Vs	B	3.258	3.446	3.566	3.647	3.702	3.818	3.878	3.908	3.929	3.946
	Vs	C	3.369	3.491	3.576	3.639	3.685	3.797	3.852	3.874	3.888	3.899
	Vs	mean	3.125	3.286	3.392	3.466	3.519	3.640	3.706	3.736	3.758	3.775
	Vp/Vs	mean	1.531	1.566	1.586	1.599	1.609	1.632	1.650	1.660	1.667	1.673
	σ	mean	0.128	0.156	0.170	0.179	0.185	0.199	0.210	0.215	0.219	0.222
A-35	Vp	A	4.564	4.843	5.020	5.145	5.239	5.488	5.688	5.802	5.884	5.949
	Vp	B	5.396	5.583	5.710	5.801	5.870	6.065	6.218	6.299	6.356	6.401
	Vp	C	6.087	6.265	6.376	6.454	6.509	6.655	6.768	6.831	6.876	6.912
	Vp	mean	5.349	5.564	5.702	5.800	5.873	6.069	6.225	6.311	6.372	6.420
	Vs	A	2.910	3.026	3.100	3.153	3.193	3.298	3.377	3.420	3.451	3.475
	Vs	B	3.615	3.676	3.716	3.745	3.769	3.834	3.882	3.905	3.922	3.934
	Vs	C	3.037	3.141	3.211	3.232	3.300	3.399	3.461	3.491	3.512	3.528
	Vs	mean	3.187	3.281	3.342	3.377	3.421	3.510	3.573	3.605	3.628	3.646
	Vp/Vs	mean	1.678	1.696	1.706	1.718	1.717	1.729	1.742	1.750	1.756	1.761
	σ	mean	0.225	0.233	0.238	0.244	0.243	0.249	0.254	0.258	0.260	0.262
A-36	Vp	A	4.122	4.677	5.042	5.294	5.472	5.859	6.055	6.150	6.219	6.273
	Vp	B	5.946	6.236	6.400	6.510	6.588	6.762	6.872	6.930	6.972	7.005
	Vp	C	5.883	6.185	6.374	6.499	6.584	6.758	6.849	6.897	6.931	6.957
	Vp	mean	5.317	5.699	5.939	6.101	6.215	6.460	6.592	6.659	6.707	6.745
	Vs	A	2.753	2.972	3.108	3.198	3.260	3.393	3.475	3.520	3.552	3.577
	Vs	B	3.743	3.843	3.908	3.951	3.980	4.042	4.074	4.094	4.102	4.111
	Vs	C	3.165	3.294	3.386	3.453	3.502	3.611	3.649	3.659	3.666	3.671
	Vs	mean	3.220	3.370	3.467	3.534	3.581	3.682	3.733	3.758	3.773	3.786
	Vp/Vs	mean	1.651	1.691	1.713	1.726	1.736	1.754	1.766	1.772	1.778	1.781
	σ	mean	0.210	0.231	0.241	0.248	0.252	0.259	0.264	0.266	0.269	0.270
A-37	Vp	A	4.197	4.709	5.028	5.241	5.389	5.730	5.971	6.109	6.210	6.289
	Vp	B	5.608	5.953	6.190	6.359	6.482	6.769	6.908	6.967	7.008	7.040
	Vp	C	5.368	5.801	6.086	6.282	6.421	6.721	6.870	6.941	6.991	7.031
	Vp	mean	5.058	5.488	5.768	5.961	6.097	6.406	6.583	6.672	6.736	6.787
	Vs	A	2.628	2.795	2.902	2.975	3.028	3.158	3.252	3.305	3.343	3.373
	Vs	B	3.530	3.708	3.826	3.907	3.964	4.083	4.135	4.158	4.173	4.186
	Vs	C	2.438	2.636	2.770	2.866	2.936	3.099	3.185	3.224	3.251	3.273
	Vs	mean	2.865	3.047	3.166	3.249	3.309	3.447	3.524	3.562	3.589	3.610
	Vp/Vs	mean	1.765	1.801	1.822	1.834	1.843	1.859	1.868	1.873	1.877	1.880
	σ	mean	0.264	0.277	0.284	0.289	0.291	0.296	0.299	0.301	0.302	0.303

Table 2. (Continued)

#	core	Pressure (MPa)										
		20	40	60	80	100	200	400	600	800	1000	
A-38	Vp	A	4.760	5.064	5.239	5.350	5.423	5.592	5.727	5.806	5.862	5.907
	Vp	B	5.982	6.080	6.141	6.185	6.219	6.321	6.414	6.467	6.505	6.534
	Vp	C	6.120	6.285	6.372	6.424	6.457	6.540	6.614	6.657	6.688	6.712
	Vp	mean	5.620	5.810	5.917	5.986	6.033	6.151	6.252	6.310	6.352	6.385
	Vs	A	3.043	3.125	3.180	3.220	3.251	3.332	3.388	3.416	3.436	3.451
	Vs	B	3.782	3.814	3.833	3.846	3.856	3.887	3.918	3.937	3.950	3.960
	Vs	C	3.642	3.744	3.780	3.798	3.810	3.846	3.883	3.904	3.920	3.932
	Vs	mean	3.489	3.561	3.598	3.621	3.639	3.688	3.730	3.752	3.769	3.781
	Vp/Vs	mean	1.611	1.631	1.645	1.653	1.658	1.668	1.676	1.682	1.685	1.689
	σ	mean	0.187	0.199	0.207	0.211	0.214	0.219	0.224	0.226	0.228	0.230
A-39	Vp	A	3.740	4.153	4.441	4.659	4.828	5.298	5.619	5.768	5.873	5.955
	Vp	B	5.250	5.551	5.753	5.901	6.012	6.306	6.505	6.604	6.675	6.730
	Vp	C	5.653	5.889	6.051	6.172	6.265	6.517	6.679	6.751	6.801	6.839
	Vp	mean	4.881	5.198	5.415	5.577	5.702	6.040	6.268	6.375	6.449	6.508
	Vs	A	2.543	2.707	2.820	2.904	2.968	3.140	3.247	3.295	3.328	3.354
	Vs	B	3.389	3.550	3.655	3.728	3.781	3.905	3.979	4.016	4.042	4.063
	Vs	C	2.647	2.775	2.865	2.934	2.989	3.145	3.250	3.293	3.321	3.343
	Vs	mean	2.860	3.011	3.113	3.189	3.246	3.397	3.492	3.535	3.564	3.587
	Vp/Vs	mean	1.707	1.727	1.739	1.749	1.757	1.778	1.795	1.803	1.810	1.815
	σ	mean	0.239	0.248	0.253	0.257	0.260	0.269	0.275	0.278	0.280	0.282
A-40	Vp	A	2.583	3.231	3.699	4.054	4.332	5.083	5.561	5.778	5.933	6.057
	Vp	B	4.151	4.644	4.984	5.234	5.423	5.911	6.213	6.355	6.455	6.535
	Vp	C	5.445	6.059	6.367	6.533	6.629	6.818	6.967	7.055	7.119	7.169
	Vp	mean	4.060	4.645	5.016	5.274	5.461	5.937	6.247	6.396	6.502	6.587
	Vs	A	2.064	2.351	2.555	2.708	2.826	3.135	3.316	3.391	3.443	3.484
	Vs	B	2.994	3.172	3.303	3.405	3.486	3.703	3.819	3.852	3.872	3.887
	Vs	C	3.145	3.335	3.452	3.530	3.584	3.706	3.790	3.837	3.871	3.898
	Vs	mean	2.734	2.953	3.104	3.215	3.299	3.515	3.641	3.694	3.729	3.757
	Vp/Vs	mean	1.485	1.573	1.616	1.641	1.656	1.689	1.715	1.732	1.744	1.753
	σ	mean	0.085	0.161	0.190	0.204	0.213	0.230	0.243	0.250	0.255	0.259
A-41	Vp	A	2.953	3.753	4.330	4.763	5.092	5.912	6.324	6.478	6.585	6.670
	Vp	B	5.087	5.538	5.865	6.119	6.324	6.918	7.315	7.467	7.564	7.638
	Vp	C	3.608	4.269	4.747	5.112	5.397	6.157	6.600	6.775	6.893	6.987
	Vp	mean	3.883	4.520	4.981	5.332	5.604	6.329	6.746	6.907	7.014	7.098
	Vs	A	2.289	2.630	2.867	3.037	3.163	3.461	3.613	3.379	3.726	3.763
	Vs	B	2.702	2.991	3.195	3.346	3.462	3.757	3.922	3.991	4.038	4.075
	Vs	C	2.305	2.604	2.816	2.973	3.092	3.384	3.528	3.582	3.619	3.648
	Vs	mean	2.432	2.742	2.959	3.119	3.239	3.534	3.688	3.651	3.794	3.828
	Vp/Vs	mean	1.597	1.649	1.683	1.709	1.730	1.791	1.829	1.892	1.849	1.854
	σ	mean	0.177	0.209	0.227	0.240	0.249	0.273	0.287	0.306	0.293	0.295

Table 2. (Continued)

#	core	Pressure (MPa)										
		20	40	60	80	100	200	400	600	800	1000	
A-42	Vp	A	3.386	4.281	4.806	5.122	5.316	5.650	5.807	5.895	5.959	6.009
	Vp	B	4.408	5.087	5.472	5.699	5.837	6.083	6.222	6.301	6.359	6.404
	Vp	C	5.232	5.722	6.000	6.167	6.271	6.469	6.596	6.669	6.722	6.763
	Vp	mean	4.342	5.030	5.426	5.662	5.808	6.067	6.208	6.288	6.346	6.392
	Vs	A	2.781	2.951	3.071	3.159	3.223	3.375	3.440	3.463	3.478	3.490
	Vs	B	3.222	3.431	3.550	3.620	3.664	3.746	3.795	3.824	3.844	3.849
	Vs	C	2.877	3.057	3.161	3.228	3.273	3.384	3.479	3.535	3.576	3.608
	Vs	mean	2.960	3.147	3.261	3.336	3.387	3.502	3.572	3.607	3.633	3.649
	Vp/Vs	mean	1.467	1.599	1.664	1.698	1.715	1.733	1.738	1.743	1.747	1.752
	σ	mean	0.066	0.179	0.217	0.234	0.242	0.250	0.253	0.255	0.256	0.258
A-43	Vp	A	3.238	4.198	4.805	5.197	5.454	5.919	6.080	6.171	6.230	6.277
	Vp	B	4.793	5.322	5.679	5.928	6.105	6.479	6.632	6.695	6.739	6.773
	Vp	C	5.440	5.864	6.148	6.345	6.484	6.779	6.904	6.958	6.996	7.025
	Vp	mean	4.490	5.128	5.544	5.824	6.014	6.392	6.539	6.608	6.655	6.692
	Vs	A	2.497	2.816	3.019	3.153	3.243	3.416	3.486	3.520	3.544	3.563
	Vs	B	3.150	3.395	3.554	3.662	3.736	3.885	3.949	3.978	3.999	4.015
	Vs	C	2.754	3.003	3.177	3.293	3.377	3.550	3.608	3.626	3.639	3.649
	Vs	mean	2.800	3.071	3.250	3.369	3.452	3.617	3.681	3.708	3.727	3.742
	Vp/Vs	mean	1.604	1.670	1.706	1.728	1.742	1.767	1.776	1.782	1.785	1.788
	σ	mean	0.182	0.220	0.238	0.248	0.254	0.265	0.268	0.270	0.271	0.272
A-44	Vp	A	2.467	3.446	4.098	4.543	4.850	5.476	5.743	5.871	5.965	6.041
	Vp	B	4.590	5.200	5.611	5.899	6.104	6.550	6.751	6.837	6.899	6.947
	Vp	C	4.996	5.507	5.850	6.087	6.254	6.610	6.765	6.832	6.879	6.916
	Vp	mean	4.018	4.718	5.186	5.510	5.736	6.212	6.420	6.513	6.581	6.635
	Vs	A	2.015	2.397	2.649	2.821	2.941	3.189	3.299	3.350	3.387	3.416
	Vs	B	2.974	3.320	3.542	3.689	3.788	3.978	4.053	4.087	4.111	4.130
	Vs	C	2.297	2.580	2.770	2.900	2.990	3.168	3.228	3.250	3.266	3.278
	Vs	mean	2.429	2.766	2.987	3.137	3.240	3.445	3.527	3.563	3.588	3.608
	Vp/Vs	mean	1.654	1.706	1.736	1.756	1.771	1.803	1.820	1.828	1.834	1.839
	σ	mean	0.212	0.238	0.252	0.260	0.266	0.278	0.284	0.287	0.289	0.290
A-45	Vp	A	3.629	4.277	4.683	4.950	5.130	5.507	5.727	5.849	5.937	6.008
	Vp	B	4.560	5.128	5.516	5.791	5.991	6.443	6.656	6.748	6.813	6.864
	Vp	C	4.951	5.369	5.671	5.898	6.074	6.521	6.747	6.823	6.872	6.911
	Vp	mean	4.380	4.925	5.290	5.547	5.732	6.157	6.377	6.473	6.541	6.594
	Vs	A	2.226	2.381	2.491	2.574	2.640	2.819	2.931	2.975	3.005	3.028
	Vs	B	2.841	3.179	3.406	3.564	3.675	6.907	3.998	4.035	4.061	4.081
	Vs	C	2.072	2.420	2.654	2.814	2.926	3.153	3.239	3.274	3.299	3.319
	Vs	mean	2.380	2.660	2.850	2.984	3.080	4.293	3.389	3.428	3.455	3.476
	Vp/Vs	mean	1.841	1.851	1.856	1.859	1.861	1.434	1.881	1.888	1.893	1.897
	σ	mean	0.291	0.294	0.295	0.296	0.297	0.027	0.303	0.305	0.307	0.308

Table 2. (Continued)

#	core	Pressure (MPa)										
		20	40	60	80	100	200	400	600	800	1000	
A-46	Vp	A	3.623	4.639	5.313	5.770	6.084	6.703	6.932	7.028	7.098	7.153
	Vp	B	3.787	4.759	5.407	5.845	6.152	6.753	6.966	7.051	7.112	7.160
	Vp	C	4.509	5.294	5.802	6.140	6.366	6.801	6.966	7.040	7.093	7.135
	Vp	mean	3.973	4.898	5.508	5.918	6.201	6.753	6.955	7.040	7.101	7.149
	Vs	A	2.505	2.957	3.252	3.450	3.583	3.841	3.933	3.972	4.000	4.021
	Vs	B	2.477	2.979	3.296	3.499	3.630	3.858	3.925	3.953	3.973	3.989
	Vs	C	2.720	3.226	3.485	3.621	3.695	3.800	3.849	3.877	3.898	3.914
	Vs	mean	2.567	3.054	3.344	3.523	3.636	3.833	3.902	3.934	3.957	3.975
	Vp/Vs	mean	1.548	1.604	1.647	1.680	1.705	1.762	1.782	1.789	1.795	1.799
	σ	mean	0.142	0.182	0.208	0.226	0.238	0.262	0.270	0.273	0.275	0.276
A-47	Vp	A	4.243	5.090	5.667	6.066	6.345	6.906	7.084	7.142	7.182	7.214
	Vp	B	3.936	4.488	5.535	5.985	6.300	6.931	7.127	7.188	7.231	7.264
	Vp	C	3.795	4.718	5.361	5.817	6.143	6.832	7.006	7.135	7.183	7.221
	Vp	mean	3.991	4.765	5.521	5.956	6.262	6.890	7.073	7.155	7.199	7.233
	Vs	A	2.683	3.118	3.396	3.577	3.695	3.904	3.964	3.988	4.005	4.018
	Vs	B	2.533	3.013	3.320	3.521	3.653	3.889	3.959	3.987	4.007	4.022
	Vs	C	2.667	3.046	3.303	3.482	3.607	3.861	3.944	3.971	3.990	4.005
	Vs	mean	2.628	3.059	3.340	3.526	3.652	3.885	3.956	3.982	4.001	4.015
	Vp/Vs	mean	1.519	1.558	1.653	1.689	1.715	1.774	1.788	1.797	1.799	1.801
	σ	mean	0.117	0.150	0.211	0.230	0.242	0.267	0.272	0.276	0.277	0.277
A-48	Vp	A	4.167	4.900	5.401	5.753	6.002	6.524	6.713	6.780	6.826	6.863
	Vp	B	3.770	4.612	5.184	5.581	5.861	6.437	6.476	6.727	6.782	6.826
	Vp	C	4.459	5.119	5.558	5.586	6.064	6.483	6.644	6.711	6.759	6.796
	Vp	mean	4.132	4.877	5.381	5.640	5.976	6.481	6.611	6.739	6.789	6.829
	Vs	A	2.490	2.939	3.221	3.402	3.520	3.730	3.803	3.836	3.860	3.879
	Vs	B	2.573	2.917	3.150	3.310	3.422	3.645	3.716	3.739	3.754	3.767
	Vs	C	2.742	3.064	3.272	3.408	3.498	3.662	3.713	3.733	3.748	3.759
	Vs	mean	2.602	2.973	3.214	3.373	3.480	3.679	3.744	3.770	3.788	3.802
	Vp/Vs	mean	1.588	1.640	1.674	1.672	1.717	1.762	1.766	1.788	1.793	1.796
	σ	mean	0.172	0.204	0.223	0.221	0.243	0.262	0.264	0.272	0.274	0.275
A-49	Vp	A	3.664	4.122	4.452	4.704	4.903	5.454	5.799	5.938	6.032	6.105
	Vp	B	4.720	5.104	5.372	5.571	5.724	6.121	6.357	6.459	6.529	6.584
	Vp	C	4.843	5.223	5.485	5.679	5.825	6.198	6.416	6.513	6.580	6.633
	Vp	mean	4.409	4.816	5.103	5.318	5.484	5.924	6.191	6.303	6.380	6.440
	Vs	A	2.535	2.748	2.897	3.008	3.093	3.316	3.450	3.508	3.549	3.580
	Vs	B	3.020	3.261	3.422	3.534	3.614	3.794	3.889	3.934	3.966	3.991
	Vs	C	3.072	3.266	3.401	3.499	3.573	3.753	3.847	3.885	3.912	3.932
	Vs	mean	2.875	3.092	3.240	3.347	3.427	3.621	3.729	3.776	3.809	3.834
	Vp/Vs	mean	1.533	1.558	1.575	1.589	1.600	1.636	1.660	1.669	1.675	1.680
	σ	mean	0.130	0.150	0.162	0.172	0.180	0.202	0.215	0.220	0.223	0.225

Table 2. (Continued)

#	core	Pressure (MPa)										
		20	40	60	80	100	200	400	600	800	1000	
A-50	Vp	A	4.107	4.587	4.917	5.153	5.325	5.715	5.897	5.972	6.025	6.067
	Vp	B	4.091	4.627	5.002	5.274	5.474	5.937	6.146	6.224	6.278	6.321
	Vp	C	4.393	4.854	5.176	5.411	5.584	5.994	6.187	6.262	6.314	6.354
	Vp	mean	4.197	4.689	5.032	5.279	5.461	5.882	6.076	6.153	6.206	6.247
	Vs	A	2.637	2.902	3.077	3.197	3.280	3.454	3.530	3.564	3.589	3.608
	Vs	B	2.656	2.983	3.197	3.343	3.444	3.647	3.731	3.768	3.794	3.815
	Vs	C	2.503	2.801	2.999	3.135	3.232	3.443	3.545	3.594	3.628	3.655
	Vs	mean	2.599	2.895	3.091	3.225	3.319	3.515	3.602	3.642	3.670	3.693
	Vp/Vs	mean	1.615	1.620	1.628	1.637	1.646	1.674	1.687	1.689	1.691	1.692
	σ	mean	0.189	0.192	0.197	0.202	0.207	0.222	0.229	0.230	0.231	0.232
A-51	Vp	A	3.563	4.129	4.542	4.857	5.101	5.734	6.064	6.176	6.279	6.307
	Vp	B	5.388	5.735	5.973	6.146	6.276	6.598	6.780	6.862	6.919	6.964
	Vp	C	4.464	4.909	5.225	5.462	5.643	6.103	6.349	6.442	6.506	6.556
	Vp	mean	4.472	4.924	5.247	5.488	5.673	6.145	6.398	6.493	6.568	6.609
	Vs	A	2.612	2.794	2.920	3.013	3.083	2.606	3.362	3.406	3.437	3.460
	Vs	B	3.117	3.341	3.490	3.594	3.667	3.827	3.903	3.938	3.963	3.982
	Vs	C	3.134	3.332	3.459	3.543	3.600	3.714	3.763	3.786	3.803	3.815
	Vs	mean	2.954	3.156	3.290	3.383	3.450	3.382	3.676	3.710	3.734	3.753
	Vp/Vs	mean	1.514	1.561	1.595	1.622	1.644	1.817	1.740	1.750	1.759	1.761
	σ	mean	0.113	0.152	0.176	0.194	0.207	0.283	0.254	0.258	0.261	0.262
A-52	Vp	A	4.253	4.787	5.150	5.412	5.604	6.067	6.325	6.447	6.533	6.601
	Vp	B	5.483	5.804	6.019	6.174	6.290	6.575	6.746	6.828	6.886	6.931
	Vp	C	5.817	6.083	6.263	6.394	6.493	6.746	6.903	6.977	7.028	7.068
	Vp	mean	5.185	5.558	5.811	5.993	6.129	6.463	6.658	6.750	6.816	6.867
	Vs	A	2.873	3.017	3.117	3.192	3.250	3.414	3.525	3.575	3.610	3.636
	Vs	B	3.447	3.550	3.362	3.677	3.721	3.850	3.941	3.978	4.002	4.020
	Vs	C	2.947	3.097	3.196	3.264	3.313	3.423	3.483	3.513	3.535	3.551
	Vs	mean	3.089	3.222	3.225	3.378	3.428	3.562	3.650	3.689	3.715	3.736
	Vp/Vs	mean	1.678	1.725	1.802	1.774	1.788	1.814	1.824	1.830	1.834	1.838
	σ	mean	0.225	0.247	0.277	0.267	0.272	0.282	0.285	0.287	0.289	0.290
A-53	Vp	A	2.955	3.855	4.490	4.951	5.290	6.070	6.419	6.557	6.654	6.732
	Vp	B	4.462	5.086	5.539	5.882	6.147	6.831	7.817	7.311	7.392	7.456
	Vp	C	4.764	5.311	5.709	6.013	6.250	6.881	7.229	7.352	7.432	7.494
	Vp	mean	4.060	4.751	5.246	5.616	5.896	6.594	7.155	7.073	7.159	7.227
	Vs	A	2.269	2.683	2.962	3.156	3.292	3.582	3.707	3.756	3.793	3.822
	Vs	B	2.953	3.285	3.514	3.679	3.799	4.073	4.197	4.245	4.279	4.306
	Vs	C	2.323	2.699	2.960	3.148	3.285	3.599	3.740	3.797	3.836	3.867
	Vs	mean	2.515	2.889	3.145	3.328	3.459	3.751	3.881	3.933	3.969	3.998
	Vp/Vs	mean	1.615	1.645	1.668	1.688	1.704	1.758	1.843	1.798	1.804	1.808
	σ	mean	0.189	0.207	0.219	0.229	0.238	0.261	0.291	0.276	0.278	0.279

Table 2. (Continued)

#	core	Pressure (MPa)										
		20	40	60	80	100	200	400	600	800	1000	
A-54	Vp	A	3.700	4.564	5.114	5.470	5.702	6.112	6.235	6.286	6.322	6.351
	Vp	B	4.744	5.399	5.831	6.124	6.324	6.721	6.870	6.932	6.976	7.011
	Vp	C	4.454	5.205	5.683	5.993	6.196	6.557	6.672	6.721	6.756	6.783
	Vp	mean	4.299	5.056	5.543	5.862	6.074	6.463	6.592	6.646	6.685	6.715
	Vs	A	2.667	2.900	3.057	3.166	3.242	3.399	3.454	3.474	3.488	3.499
	Vs	B	2.999	3.266	3.442	3.561	3.642	3.803	3.862	3.887	3.904	3.917
	Vs	C	2.644	2.886	3.048	3.160	3.238	3.400	3.462	3.486	3.503	3.516
	Vs	mean	2.770	3.017	3.182	3.295	3.374	3.534	3.593	3.616	3.632	3.644
	Vp/Vs	mean	1.552	1.676	1.742	1.779	1.800	1.829	1.835	1.838	1.841	1.843
	σ	mean	0.145	0.224	0.254	0.269	0.277	0.287	0.289	0.290	0.291	0.291
A-55	Vp	A	3.025	3.661	4.104	4.427	4.669	5.262	5.597	5.753	5.866	5.955
	Vp	B	4.606	5.054	5.364	5.590	5.759	6.174	6.399	6.497	6.566	6.619
	Vp	C	4.724	5.107	5.368	5.560	5.704	6.068	6.285	6.385	6.456	6.511
	Vp	mean	4.118	4.607	4.945	5.192	5.377	5.835	6.094	6.212	6.296	6.362
	Vs	A	2.115	2.470	2.713	2.887	3.013	3.306	3.457	3.526	3.575	3.614
	Vs	B	2.822	3.092	3.275	3.404	3.498	3.706	3.803	3.845	3.874	3.894
	Vs	C	2.122	2.426	2.643	2.802	2.921	3.204	3.332	3.377	3.407	3.420
	Vs	mean	2.353	2.663	2.877	3.031	3.144	3.405	3.531	3.582	3.619	3.642
	Vp/Vs	mean	1.750	1.730	1.719	1.713	1.710	1.713	1.726	1.734	1.740	1.747
	σ	mean	0.258	0.249	0.244	0.242	0.240	0.242	0.247	0.251	0.253	0.256
A-79	Vp	A	3.448	4.131	4.616	4.971	5.235	5.857	6.136	6.238	6.308	6.363
	Vp	B	4.473	5.070	5.485	5.785	6.004	6.506	6.729	6.815	6.875	6.922
	Vp	C	4.756	5.225	5.566	5.824	6.023	6.531	6.781	6.862	6.914	6.954
	Vp	mean	4.226	4.809	5.222	5.527	5.754	6.298	6.549	6.638	6.699	6.746
	Vs	A	2.526	2.816	3.015	3.156	3.258	3.491	3.601	3.648	3.680	3.061
	Vs	B	2.831	3.125	3.327	3.469	3.572	3.802	3.904	3.946	3.975	3.998
	Vs	C	2.150	2.367	2.519	2.629	2.712	2.908	3.004	3.041	3.067	3.088
	Vs	mean	2.502	2.770	2.953	3.085	3.181	3.400	3.503	3.545	3.574	3.382
	Vp/Vs	mean	1.689	1.736	1.768	1.792	1.809	1.852	1.870	1.873	1.874	1.994
	σ	mean	0.230	0.252	0.265	0.274	0.280	0.294	0.300	0.301	0.301	0.332
A-90	Vp	A	3.164	3.434	3.612	3.747	6.859	4.230	4.611	4.821	4.964	5.074
	Vp	B	4.816	4.983	5.093	5.176	5.244	5.459	5.653	5.748	5.810	5.857
	Vp	C	5.017	5.223	5.342	5.423	5.484	5.668	5.853	5.964	6.044	6.107
	Vp	mean	4.332	4.546	4.682	4.782	5.862	5.119	5.372	5.511	5.606	5.679
	Vs	A	2.067	2.207	2.297	2.364	2.417	2.577	2.722	2.803	2.862	2.908
	Vs	B	2.975	3.103	3.185	3.247	3.288	3.412	3.514	3.571	3.613	3.645
	Vs	C	3.271	3.344	3.394	3.433	3.464	3.555	3.620	3.648	3.666	3.679
	Vs	mean	2.771	2.885	2.959	3.015	3.056	3.181	3.285	3.341	3.380	3.411
	Vp/Vs	mean	1.564	1.576	1.582	1.586	1.918	1.609	1.635	1.650	1.659	1.665
	σ	mean	0.154	0.163	0.168	0.170	0.313	0.185	0.201	0.209	0.214	0.218

Table 2. (Continued)

#	core	Pressure (MPa)										
		20	40	60	80	100	200	400	600	800	1000	
A-301	Vp	A	5.344	5.436	5.490	5.530	5.563	5.672	5.790	5.860	5.910	5.949
	Vp	B	5.198	5.301	5.364	5.411	5.449	5.575	5.712	5.793	5.847	5.888
	Vp	C	5.179	5.293	5.361	5.411	5.451	5.581	5.725	5.818	5.888	5.945
	Vp	mean	5.240	5.343	5.405	5.451	5.488	5.609	5.742	5.824	5.882	5.927
	Vs	A	3.192	3.227	3.247	3.261	3.273	3.309	3.349	3.372	3.389	3.402
	Vs	B	3.176	3.204	3.221	3.235	3.246	3.287	3.338	3.373	3.400	3.420
	Vs	C	3.171	3.204	3.225	3.241	3.255	3.302	3.352	3.381	3.402	3.419
	Vs	mean	3.180	3.212	3.231	3.246	3.258	3.299	3.346	3.375	3.397	3.414
	Vp/Vs	mean	1.648	1.664	1.673	1.679	1.684	1.700	1.716	1.725	1.731	1.736
	σ	mean	0.209	0.217	0.222	0.225	0.228	0.236	0.243	0.247	0.250	0.252
A-302	Vp	A	3.562	3.876	4.097	4.269	4.407	4.824	5.139	5.277	5.368	5.438
	Vp	B	3.912	4.212	4.398	4.454	4.654	4.999	5.271	5.398	5.483	5.550
	Vp	C	3.803	4.089	4.286	4.437	4.557	4.912	5.180	5.304	5.389	5.455
	Vp	mean	3.769	4.059	4.260	4.387	4.539	4.912	5.197	5.326	5.413	5.481
	Vs	A	2.394	2.525	2.613	2.678	2.729	2.874	2.981	3.034	3.072	3.101
	Vs	B	2.446	2.567	2.651	2.714	2.764	2.900	2.990	3.029	3.056	3.077
	Vs	C	2.509	2.611	2.679	2.731	2.772	2.895	2.990	3.036	3.066	3.090
	Vs	mean	2.450	2.568	2.648	2.708	2.755	2.890	2.987	3.033	3.065	3.089
	Vp/Vs	mean	1.539	1.581	1.609	1.620	2.011	1.700	1.740	1.756	1.766	1.774
	σ	mean	0.134	0.166	0.185	0.192	0.336	0.235	0.253	0.260	0.264	0.267
A-303	Vp	A	5.328	5.391	5.433	5.466	5.494	5.587	5.679	5.724	5.750	5.768
	Vp	B	5.414	5.519	5.580	5.621	5.650	5.731	5.804	5.848	5.879	5.903
	Vp	C	5.343	5.408	5.451	5.483	5.551	5.602	5.691	5.734	5.761	5.780
	Vp	mean	5.362	5.439	5.488	5.523	5.565	5.640	5.725	5.769	5.797	5.817
	Vs	A	3.179	3.200	3.211	3.219	3.225	3.245	3.270	3.287	3.300	3.309
	Vs	B	3.301	3.312	3.321	3.329	3.335	3.353	3.359	3.359	3.358	3.356
	Vs	C	3.178	3.197	3.211	3.223	3.232	3.258	3.272	3.276	3.278	3.280
	Vs	mean	3.219	3.236	3.248	3.257	3.264	3.285	3.300	3.307	3.312	3.315
	Vp/Vs	mean	1.665	1.681	1.690	1.696	1.705	1.717	1.735	1.744	1.750	1.755
	σ	mean	0.218	0.226	0.231	0.233	0.238	0.243	0.251	0.255	0.258	0.260

Note: seismic velocities in km/sec, Vp/Vs and Poisson (σ) ratios are dimensionless. For densities see Table 1.

Typical velocity-pressure curves are shown in Figure 1 for a high-grade Alpine schist (A-1), two low-grade greywackes (A-302 and A-23) and Darran gabbro (A-46). These characteristic curves of velocity versus pressure show rapid decreases in slope at pressures near 100 MPa and approximate linearity at pressures between 400 and 1000 MPa. The initial steep slopes for the gabbro demonstrate that the rock from which the cores were extracted contained abundant microcracks. Many of these cracks may have originated from

hammering on the massive gabbro outcrop during the sample collection process.

COMPARISONS WITH PUBLISHED LABORATORY AND FIELD MEASUREMENTS

Classification schemes for most rocks allow for fairly wide ranges in mineralogy for a specific rock type, resulting in significant ranges in physical properties. This is especially

true for metamorphic rocks classified according to facies, which can have a wide variability in parent rock chemistries. Many of the rocks included in Tables 1–3 are metamorphic, ranging in grade from zeolite to amphibolite facies. The following discussion concentrates on two of the major South Island lithologies, the relatively high grade garnet-bearing Haast schist and the Torlesse greywacke.

In the Eastern subprovince some of the highest grade quartzofeldspathic mica schists are of amphibolite facies grade and often contain garnet and oligoclase. At 600 MPa, a mid crustal pressure, compressional wave velocities for the eight samples of schist (samples A-1 through A-5, A-10 through A-12) from the garnet zone range from 6.09 to 6.25 km/s and average 6.19 km/s (Table 2). The average density of these rocks is 2710 kg/m³. Garnet is not abundant in these rocks and averages only about 1% by volume. At a similar pressure *Birch* [1960] reported a mean compressional wave velocity of 6.59 km/s and a density of 2800 kg/m³ for a garnet schist from Woodsville, Vermont, and *Christensen* [1965] found a mean velocity of 6.50 km/s and a density of 2760 kg/m³ for a garnet schist from Thomaston, Connecticut. Both of these are higher in velocity and density than the New Zealand schists. The differences appear to be due to higher garnet content (approximately 5%) within the Vermont and Connecticut samples.

Based on laboratory measurements, *Hughes et al.* [1993] reported a compressional wave velocity of 6.21 km/s at 600 MPa and a density of 2686 kg/m³ for a garnet schist from Lincoln Gap, Vermont, in excellent agreement with the average New Zealand samples. *Iida et al.* [1967] measured compressional wave velocities ranging from 6.10 to 6.45 km/s for 12 garnet-bearing quartz mica schists from Japan. The

mean velocity of this suite (6.30 km/s) and density (2730 kg/m³) are in reasonable agreement with the New Zealand garnet schists.

Comparisons of the garnet-bearing Haast schist velocities with seismically measured velocities in South Island New Zealand are possible due to several recent field studies. The garnet schists are likely to be in equilibrium at mid crustal depths. *Davey et al.* [1998] found a velocity of 6.2 km/s for the midcrust (20 km depth) of the Western subprovince of New Zealand. This velocity is similar to the 6.2 to 6.4 km/s velocities at 20 km reported by *Eberhart-Phillips* [1995] and *Leitner et al.* [2001] based on passive seismic studies and by *Scherwath et al.* [2003] and *van Avendonk et al.* [2004] based on active-source seismic profiling. These values are all in reasonable agreement with the laboratory measurements of garnet-bearing quartz mica schists at 600 MPa summarized above.

Torlesse rocks are major constituents of New Zealand, occupying approximately a quarter of the surface of South Island (Plate 1). In eastern South Island the Torlesse consists of marine clastic sediments with less common interlayered basaltic lava, tuffaceous sediments and limestone. The thickness of the Torlesse is unknown, but probably significant because of its widespread distribution. Compressional wave velocities measured for seven Torlesse greywackes (samples A-21 through A-25, A-31B, A-32B; Table 2) average 6.08 km/s at 100 MPa. The average density is 2704 kg/m³. *Birch* [1960] reported a slightly lower velocity and density of 5.87 km/s and 2679 kg/m³ for a New Zealand greywacke. The specific locality of this sample was not given. Velocities at 100 MPa and densities for greywacke from the Valdez Group in Southern Alaska of 6.17 km/s and 6.12 km/s and 2767 kg/m³ and 2716 kg/m³ [*Fuis et al.*, 1991; *Brocher et al.*, 1989] are similar to the Torlesse samples. An average compressional wave velocity of 5.89 km/s at 100 MPa, and density of 2738 kg/m³ for a suite of ten California greywackes [*Stewart and Peselnick*, 1977] are also in reasonable agreement with the New Zealand samples, considering the variable mineralogy common to greywackes.

Recent field based measurements of seismic velocities below exposures of Torlesse are in good agreement with the laboratory measurements of greywacke in Table 2. Near surface velocities are quite low, presumably due to fracturing. However at depths of a few kilometers crustal velocities appear to be comparable to that of fracture free Torlesse greywacke. Modeling of both explosion and onshore-offshore data by *Davey et al.* [1998] gives a velocity of 5.9 km/s at 5 to 10 km depths. At similar depths *Leitner et al.* [2001] found velocities of 6.1 km/s. *Eberhart-Phillips et al.* [2001] measured velocities in Torlesse of 6.1 km/s at depths below 1 km.

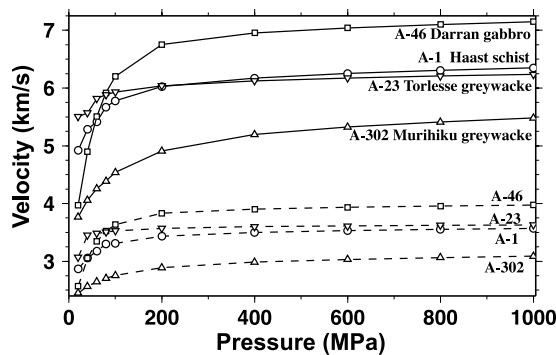


Figure 1. Measured acoustic velocities for representative samples. Solid lines are mean compressional velocity; dashed lines are mean shear velocities. Mean velocities determined by averaging of measurements in principal directions. See Table 2 for velocity numerical values.

Table 3. Whole rock chemical analyses in weight percent. Digital version of this table is on the CDROM which accompanies this volume.

	SiO ₂	TiO ₂	Al ₂ O ₃	Fe ₂ O ₃ *	MgO	CaO	MnO	Na ₂ O	K ₂ O	P ₂ O ₅	H ₂ O†	Total
A-1	68.71	0.69	15.37	5.36	1.72	1.55	0.08	2.86	2.95	0.15	1.20	100.65
A-2	64.16	0.70	16.73	6.88	1.99	1.83	0.07	2.59	3.77	0.19	1.80	100.73
A-3	70.03	0.65	14.96	4.76	1.46	1.51	0.07	2.71	3.03	0.11	1.50	100.80
A-4	73.55	0.51	12.89	3.86	1.06	2.41	0.07	3.68	1.06	0.10	0.70	99.90
A-5	62.90	0.79	17.72	6.31	1.79	1.31	0.07	2.12	3.79	0.14	3.70	100.65
A-6	73.61	0.57	10.65	6.76	2.01	1.11	0.06	1.40	2.84	0.14	0.50	99.67
A-7	74.81	0.57	11.94	4.23	1.53	0.18	0.05	1.33	2.78	0.13	2.10	99.66
A-8	62.41	0.73	18.45	6.16	2.57	0.28	0.05	0.16	5.09	0.11	4.50	100.52
A-9	69.18	0.57	12.52	5.68	1.96	3.14	0.11	2.16	2.42	0.14	2.80	100.69
A-10	70.25	0.57	14.62	4.97	1.63	1.75	0.05	2.92	2.84	0.13	0.80	100.54
A-11	70.03	0.58	15.19	4.21	1.38	1.54	0.06	2.81	3.44	0.14	1.20	100.59
A-12	62.57	0.83	17.82	6.39	2.27	2.22	0.04	3.65	3.32	0.18	1.40	100.70
A-13	72.74	0.47	13.51	3.96	1.30	1.07	0.04	3.25	2.47	0.11	1.50	100.43
A-14	74.49	0.41	13.00	3.09	0.91	1.38	0.04	3.11	2.66	0.06	1.40	100.55
A-15	69.92	0.57	13.99	5.11	1.36	1.82	0.09	3.89	1.74	0.23	1.90	100.62
A-16	65.36	0.78	16.17	6.48	1.84	1.22	0.06	2.70	2.66	0.18	2.80	100.26
A-17	68.44	0.63	14.64	4.84	1.60	2.32	0.08	3.81	1.87	0.16	2.10	100.50
A-18	70.03	0.56	13.94	4.26	1.50	2.61	0.07	3.75	1.93	0.14	1.40	100.20
A-19	69.21	0.57	14.55	4.92	1.48	2.21	0.07	3.81	1.89	0.10	1.70	100.52
A-20	74.59	0.46	12.20	3.59	0.95	1.15	0.05	2.38	2.65	0.07	1.60	99.70
A-21	67.45	0.57	14.02	5.93	1.58	2.37	0.06	3.41	2.63	0.13	1.40	99.56
A-22	69.82	0.44	14.11	5.15	1.05	1.74	0.06	3.71	2.74	0.09	0.60	99.52
A-23	71.55	0.50	13.19	5.73	1.31	1.12	0.06	3.43	2.28	0.09	1.10	100.38
A-24	73.10	0.34	13.90	3.05	0.78	1.56	0.04	4.12	2.53	0.09	1.00	100.53
A-25	68.24	0.47	13.97	7.20	1.53	1.76	0.07	3.14	3.05	0.12	1.00	100.57
A-26	53.42	0.06	2.78	6.53	22.28	10.54	0.19	0.20	0.21	0.09	3.20	99.74
A-28	72.25	0.27	14.16	2.20	0.56	1.14	0.03	3.94	4.12	0.11	1.00	99.80
A-29	71.11	0.38	14.09	3.07	0.85	2.10	0.04	2.66	4.77	0.10	0.40	99.57
A-30	70.08	0.57	13.63	4.64	2.13	1.76	0.06	3.39	2.14	0.12	1.90	100.44
A-31B	69.27	0.44	14.66	4.56	1.27	1.70	0.06	3.48	3.09	0.13	1.20	99.87
A-32B	66.19	0.87	14.49	7.29	2.06	2.89	0.10	3.35	1.36	0.18	1.70	100.49
A-33	70.65	0.49	13.88	4.35	1.13	1.45	0.05	4.51	1.73	0.13	1.60	99.98
A-34	71.50	0.41	13.23	3.83	1.13	2.26	0.06	3.80	2.20	0.08	1.30	99.81
A-35	69.20	0.46	14.13	3.90	1.02	2.65	0.06	3.33	2.77	0.12	1.40	99.04
A-36	61.43	0.78	15.54	6.65	2.70	4.47	0.09	4.02	1.62	0.10	2.40	99.81
A-37	63.07	0.75	14.98	6.74	2.43	3.70	0.10	3.62	1.83	0.11	2.20	99.54
A-38	64.48	0.62	15.97	6.69	1.57	1.66	0.09	2.14	4.38	0.12	1.90	99.63
A-39	60.09	0.79	17.11	6.83	2.54	2.85	0.07	3.12	2.79	0.15	2.60	98.94
A-40	67.09	0.55	15.41	4.59	1.70	1.85	0.06	3.93	2.63	0.16	2.10	100.07
A-41	48.01	2.83	14.52	12.65	5.86	9.75	0.18	3.54	0.15	0.34	2.20	100.05
A-42	68.50	0.53	14.28	5.14	1.59	1.51	0.07	3.28	2.92	0.10	2.10	100.03
A-43	63.91	0.69	14.30	6.31	2.21	3.09	0.10	5.17	1.33	0.16	1.60	98.88
A-44	64.26	0.79	16.07	6.27	1.99	1.73	0.20	2.83	3.12	0.16	2.40	99.82

Table 3. (Continued)

	SiO ₂	TiO ₂	Al ₂ O ₃	Fe ₂ O ₃ *	MgO	CaO	MnO	Na ₂ O	K ₂ O	P ₂ O ₅	H ₂ O†	Total
A-45	63.94	0.78	16.02	6.40	1.95	1.51	0.09	2.84	3.04	0.17	2.20	98.95
A-46	51.30	0.73	19.36	8.08	5.55	10.17	0.12	3.41	0.21	0.08	0.50	99.52
A-47	44.51	1.17	16.38	13.87	8.25	11.86	0.13	1.68	0.33	0.10	1.50	99.79
A-48	53.65	0.93	17.20	8.83	5.25	8.17	0.13	3.46	1.14	0.14	0.20	99.11
A-49	65.63	0.63	14.67	5.41	2.07	3.30	0.07	3.37	1.84	0.13	2.00	99.12
A-50	70.01	0.40	13.58	4.91	1.73	2.61	0.08	3.83	1.72	0.12	0.60	99.60
A-51	59.89	0.82	16.66	6.85	3.07	2.91	0.10	4.51	1.38	0.22	2.50	98.92
A-52	44.84	2.96	14.10	16.55	6.52	8.36	0.17	2.42	0.13	0.34	3.60	100.00
A-53	46.95	2.81	15.54	12.35	4.50	12.08	0.13	2.98	0.23	0.35	2.00	99.93
A-54	43.45	3.47	13.92	14.45	5.30	7.46	0.15	3.10	0.42	0.37	7.90	100.00
A-55	64.08	0.83	16.75	5.86	1.89	1.43	0.07	3.03	3.13	0.14	2.70	99.92
A-79	46.74	2.11	19.16	14.63	3.04	7.74	0.36	3.44	1.11	0.22	1.50	100.09
A-90	63.30	0.67	17.10	5.69	1.49	0.62	0.06	2.75	3.49	0.12	4.30	99.60
A-301	64.06	0.69	15.66	7.82	2.01	1.48	0.08	3.14	2.02	0.17	2.60	99.74
A-302	59.10	0.86	16.68	7.14	2.74	2.73	0.09	3.93	1.67	0.12	4.70	99.77
A-303	67.32	0.50	14.14	7.60	0.96	1.41	0.07	2.74	3.41	0.09	2.15	100.40

*Total iron as Fe₂O₃.

†Loss on ignition for ICP analyses.

VELOCITY-DENSITY AND VELOCITY-CHEMISTRY SYSTEMATICS

Relationships between seismic velocity and density have important implications for multidisciplinary geophysical studies involving seismic and gravity investigations [e.g., *Birch*, 1960; *Brocher*, 2005]. Velocity-density correlations can be useful in the determination of velocity from gravity data or vice versa. These relationships can also be used to estimate lithology from either gravity or seismic data. Velocity-density relationships also provide information about the acoustic impedances of different rock types, which are important in the interpretation of reflection seismic data.

The following discussion is limited to rocks from the Torlesse Supergroup and the Haast Schist Group, which make up much of the Southern Alps of New Zealand and have been the subject of several recent seismic investigations [see *Davey et al.*, this volume]. These rocks have parent lithologies ranging from sandstone, siltstone and shale to mafic volcanics and volcanoclastic sediments. Metamorphic grade ranges from prehnite-pumpellyite through pumpellyite-actinolite facies and greenschist facies to amphibolite facies. The lowest grade rocks occur in the Torlesse. The Haast Schist Group has been divided into three mineralogic zones [e.g., *Landis and*

Coombs, 1967]; a Chlorite Zone, Biotite Zone and Garnet-Oligoclase Zone (Plate 1). The Chlorite Zone has in turn been subdivided into subzones II, III and IV. Torlesse rocks grade into subzone II rocks and subzone IV rocks grade into the Biotite Zone.

Velocities at 600 MPa are shown versus density in Figure 2. Compressional wave velocities show a steady increase with increasing density with a relatively low density (2600 to 2800 kg/m³) cluster of metasediments. The higher density points are mafic volcanic rocks from the Caples Terrane. These mafic rocks have significantly higher acoustic impedances and thus if of sufficient thickness should produce strong reflections when interlayered with metasediments. The slope of the shear wave velocity-density least squares fit is much lower. This is due to the high shear wave velocity of quartz, which is abundant in the metasediments. In Figure 3 we have plotted velocity versus density at 600 MPa for the metasedimentary rocks (exclusive of metavolcanics) of the Torlesse and Haast. The metamorphic grade of each data point is labeled. An important finding here is that there is little correlation between metamorphic grade and velocity or density for these rocks (see Figure 1; *Godfrey et al.* [2000]). Part of this is due to their chemical similarities (Table 3). Thus seismic studies will be unable to distinguish between the various subdivisions of the Haast Schist.

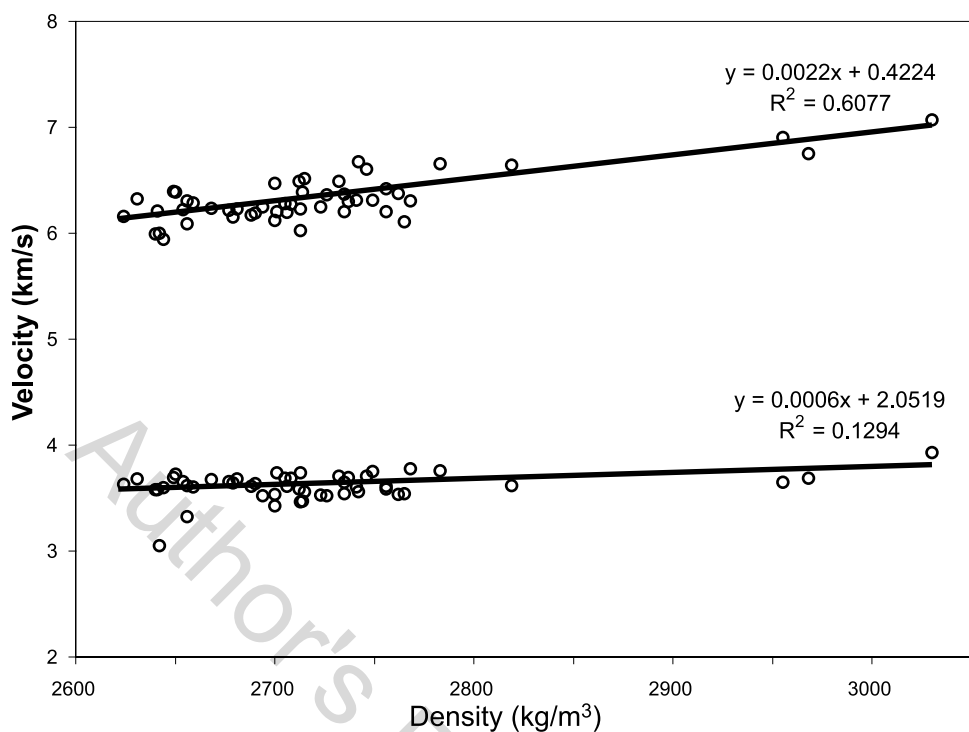


Figure 2. Compressional and shear wave velocities at 600 MPa plotted against density for rocks from the Torlesse Supergroup and the Haast Schist Group. The higher velocity rocks are metamorphosed mafic volcanics. Linear regression lines and parameters are shown in the figure.

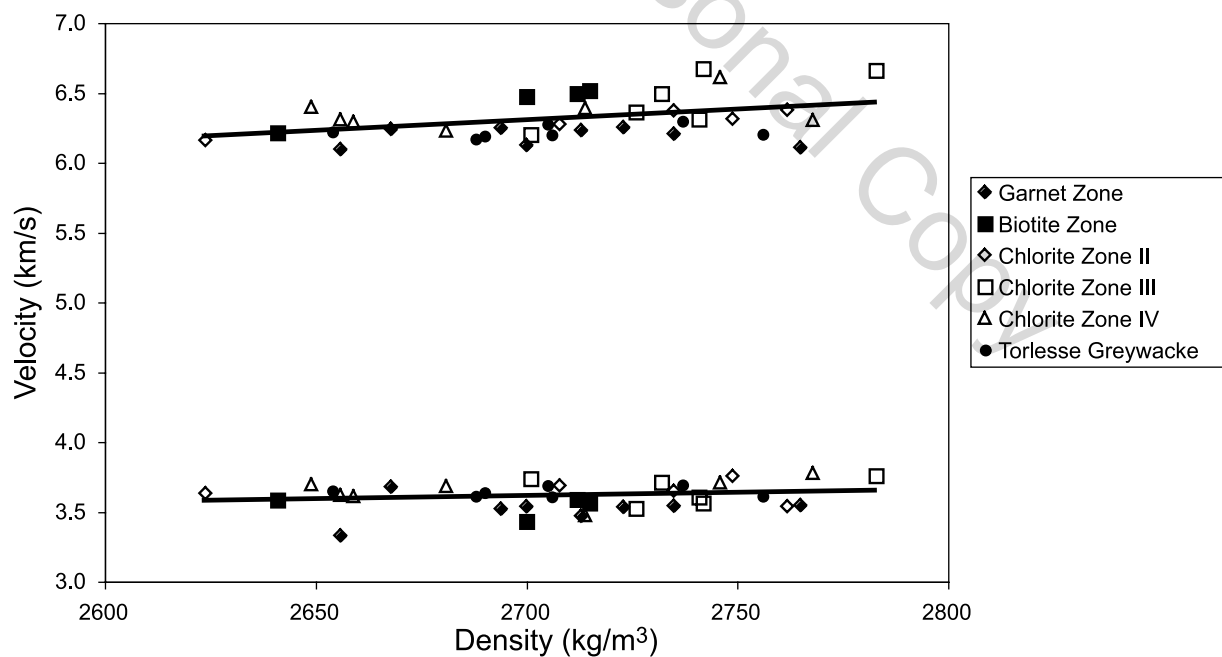


Figure 3. Compressional and shear wave velocities at 600 MPa plotted against density for metasedimentary rocks from the Torlesse Supergroup and the Haast Schist Group. The Haast Schist rocks are separated according to metamorphic grade. There is little correlation between metamorphic grade and velocity or density for these rocks.

Whole rock geochemical analyses for the rocks in Table 3 were made by Acme Analytical Laboratories, Vancouver, British Columbia, by inductively coupled plasma (ICP) analyses.

Beginning with the pioneering work of *Birch* [1961], several studies have attempted to correlate velocity with various geochemical parameters. Igneous complexes which have undergone differentiation such as the Kohistan Arc [*Miller and Christensen*, 1994] seem to show the best correlations. Some metasedimentary sequences such as phyllonites from the Brevard fault zone in North Carolina show a simple relationship between velocity and SiO_2 content [*Christensen and Szymanski*, 1988]. This correlation is evident in a plot of velocity versus weight percent SiO_2 of samples from the Torlesse and Haast Schist (Figure 4). As with the velocity-density relation, the mafic volcanics are separated from the metasediments and the slope of the shear wave velocity-% SiO_2 relation is practically flat. Note also that SiO_2 contents vary widely within the various metamorphic zones (Figure 5).

Another geochemical index that shows significant correlation with velocities of the Torlesse and Haast Schist is Mg number (Mg#), which is calculated from the mole proportion Mg divided by the sum of the mole proportion Mg + mole proportion Fe. In Figure 6 it can be seen that increasing

Fe content (decreasing Mg#) correlates with decreasing compressional wave velocity. Shear wave velocity shows no correlation with Mg#. Also the Torlesse samples seem to have lower Mg#'s than the Haast Schists and samples of Haast Schist of similar metamorphic grade often show wide ranges in Mg#.

Poisson's Ratio and V_p/V_s

Often various rock elastic parameters such as the bulk modulus, compressibility and Poisson's ratio are of interest in geophysics. With the formulas of isotropic elasticity [*Birch*, 1960] any two elastic parameters can be used to calculate all others. The elastic parameters also exhibit a functional relationship to compressional and shear wave velocities and rock density.

Poisson's ratio, calculated from V_p/V_s , has been shown to be an important parameter for determining crustal composition [e.g., *Christensen*, 1996]. Values of V_p/V_s and Poisson's ratio are given in Table 1. The mean V_p for three directions has been combined with the mean V_s of the rock samples to obtain the calculated values. The Poisson's ratios in Table 1 are more reliable for the rock samples with relatively low anisotropies. For the highly anisotropic rocks the data are

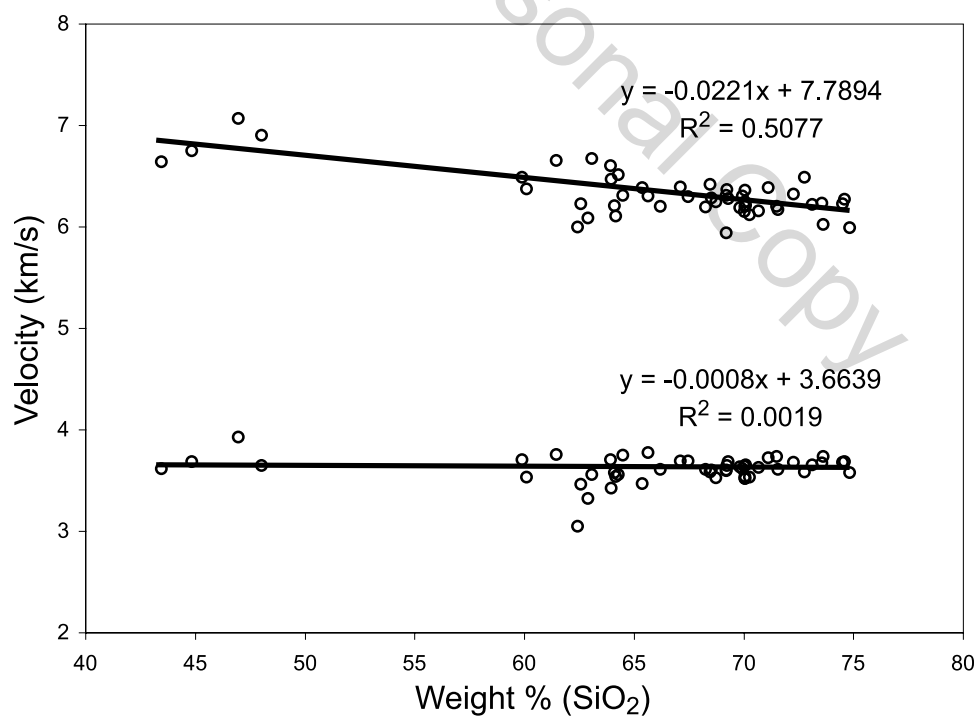


Figure 4. Compressional and shear wave velocities at 600 MPa plotted versus whole rock wt% SiO_2 . The four rocks with SiO_2 contents of 40 to 50% are metamorphosed mafic volcanics.

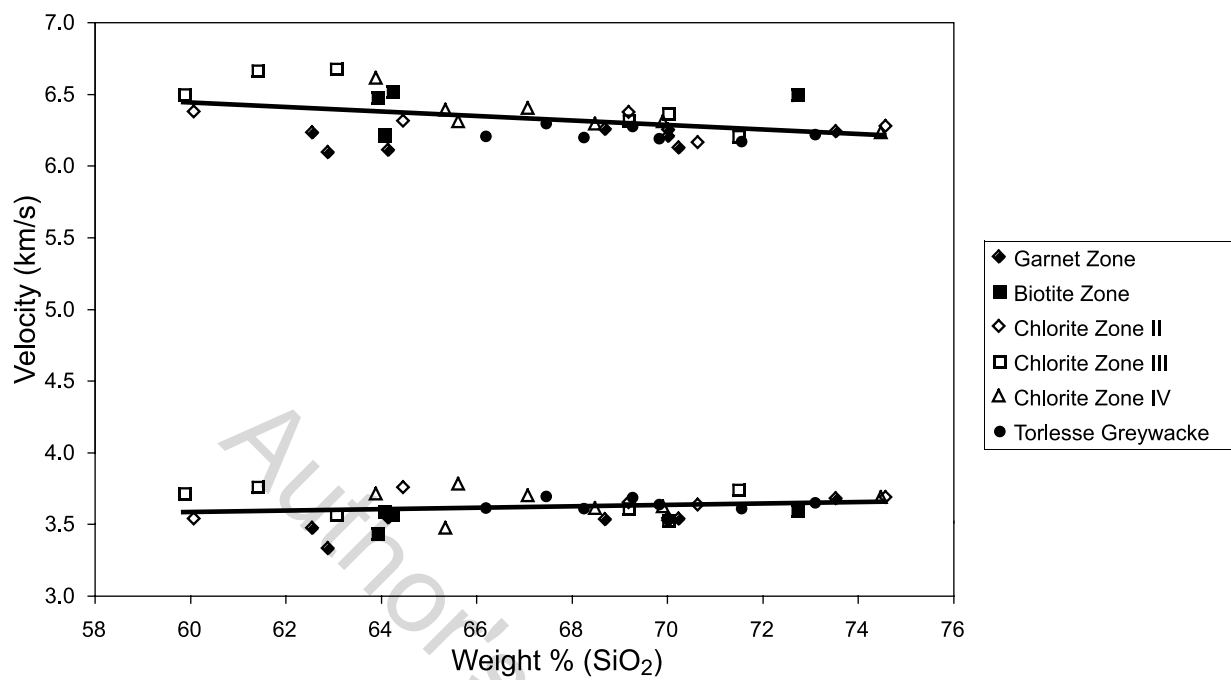


Figure 5. Compressional and shear wave velocities at 600 MPa plotted against whole rock wt% SiO₂ for metasedimentary rocks from the Torlesse Supergroup and the Haast Schist Group. The Haast Schist rocks are separated according to metamorphic grade.

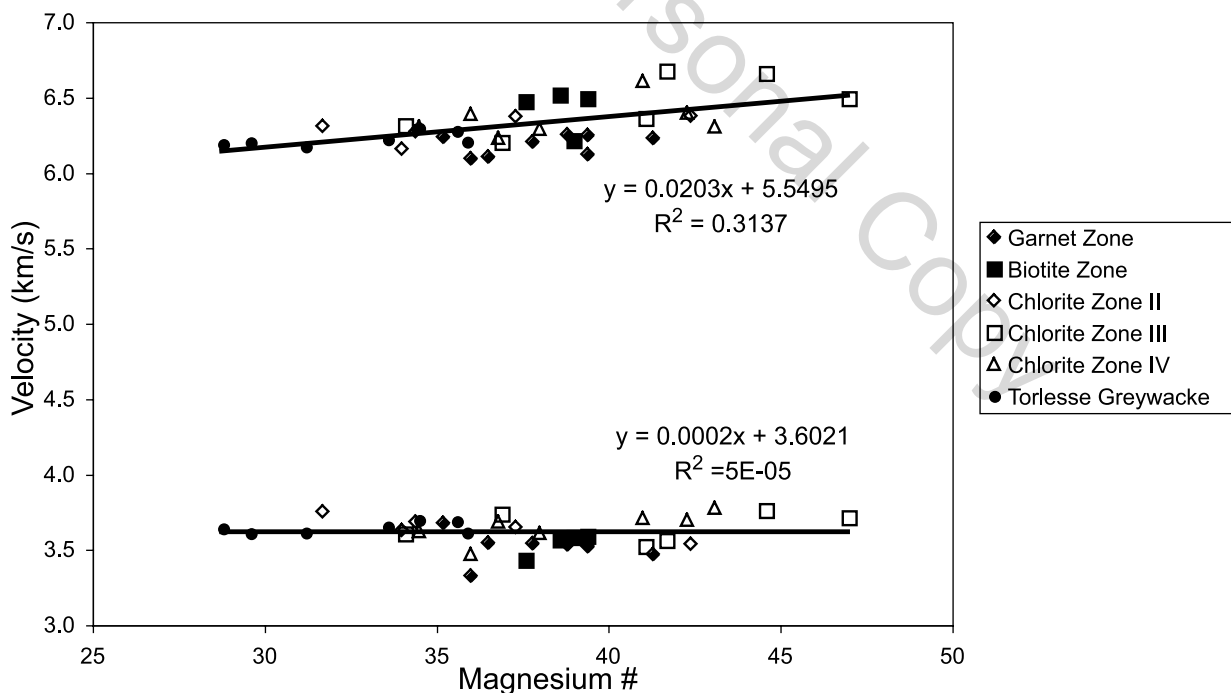


Figure 6. Laboratory measured compressional and shear wave velocities at 600 MPa plotted against whole rock magnesium number (mole proportion Mg/ mole proportion Mg + mole proportion Fe) for metasedimentary rocks from the Torlesse Supergroup and the Haast Schist Group.

presumably representative of rocks with similar mineralogy but a random mineral orientation.

The lithologies of Table 1 with the lowest anisotropies include granite, gabbro and greywacke. At high pressures, where microcracks are closed, the Tuhua granite samples (A-28 and A-29) have Poisson's ratios between 0.24 and 0.25. This compares favorably with an average of 0.24 at similar pressures for 38 granites reported by Christensen [1996]. The three gabbros in Table 1 (A-46, A-47 and A-48) have Poisson's ratios at high pressures between 0.28 and 0.29, in good agreement with Christensen's 0.296 average for 58 gabbroic rocks. The seven samples of Torlesse greywacke have Poisson's ratios at high pressures of 0.24 to 0.25 compared to a slightly higher 0.26 average for 36 samples in Christensen's compilation.

ELASTIC ANISOTROPY AND ROCK FABRIC

Seismic anisotropy is an important property of the rocks from the Haast Schist Terrane. This has been covered in detail in earlier papers [Okaya *et al.*, 1995; Godfrey *et al.*, 2000, 2002; Okaya and Christensen, 2002] and will only be briefly addressed here.

The three propagation directions listed in Table 2 for each sample provide information on maximum compressional wave anisotropy. Minimum velocities were measured normal to foliations (A core). Maximum compressional wave velocities were recorded for propagation in the foliations (B and C cores), usually parallel to lineations, if present. The shear wave velocities for the B and C cores give an estimate of maximum shear wave splitting for most rocks. As was discussed earlier, the B core shear wave velocities were measured with propagation and vibration directions parallel to foliations, whereas C core shear wave velocities were measured with propagations in the foliations and vibration directions normal to foliations. The results of these measurements, summarized by Godfrey *et al.* [2002], are shown in Figure 7.

Petrographic examinations of thin sections prepared from the sample core ends show that mineral preferred orientations (principally layer lattice silicates) are primarily responsible for the observed anisotropy. Since this anisotropy persists at high pressures, it is not related to crack orientation. The magnitudes of the anisotropies in Figure 7 are consistent with laboratory anisotropy measurements of similar rocks from other localities [e.g., Christensen, 1965, 1966; Ji and Salisbury, 1993; Kern and Wenk, 1990].

The overall symmetries of the New Zealand rocks are of prime significance in understanding their seismic anisotropies. Symmetries of rock fabrics are quite similar to those of single crystals and both can be defined in terms of point-group symmetries. Many of the metamorphic rocks included

in this study have well developed foliations and cleavages related to preferred mineral orientations. Symmetry of these rocks often approximate axial, with symmetry axes normal to the foliation or cleavage. Their elastic properties are similar to hexagonal crystals with five independent elastic constants with similar velocities for all directions of propagation within the foliation or cleavage.

Often foliations show associated linear elements. Several lineations have been observed in the New Zealand rocks including lineations formed by intersecting foliations, stretching of grains, lineations defined by the preferred orientation of elongate amphibole and crenulations of the foliation planes. For the micaceous rocks included in this study crenulation lineations are the most common, whereas lineations in the amphibolites originate from preferred orientation of prismatic hornblende. The elasticity of the lineated rocks often approximates that of orthorhombic single crystals with nine independent elastic constants. This is evident for samples in Table 2 where the velocities are different in orthogonal directions within the foliation or cleavage planes. Fast compressional wave velocities parallel the lineations.

The velocity data of Table 2 demonstrates that several rock types are, to a first approximation, isotropic. These include Tuhua granite, Torlesse greywacke, Murihiku greywacke, and Mackay gabbro. As expected, the most highly anisotropic samples are from the Alpine and Otago schist belts. Symmetries of the schists and greenschists vary from axial (samples A-1 through A-4, A-36, A-37, A-44, A-49) to orthorhombic (A-5, A-8, A-12 through A-15, A-19, A-35, A-38, A-40, A-42, A-43, A-51). The amphibolites also show axial symmetry (A-52, A-53, A-79) and orthorhombic symmetry (A-41, A-54). A complete transition from pure axial symmetry (only a foliation) to robust orthorhombic symmetry (a well-developed lineation) exists in the data suite, as shown by the magnitudes of the anisotropies (Table 2).

The velocity measurements presented in Table 2 provide details of wave propagation along major symmetry directions and usually give maximum P wave anisotropy and S wave splitting. Velocity measurements in non-symmetry directions are required to calculate complete three-dimensional velocity surfaces [Auld, 1990; Johnston and Christensen, 1995; Godfrey *et al.*, 2000]. For rocks with axial symmetry, quasi-compressional wave velocity measurements are required in one direction at 45 degrees to the symmetry axis, whereas measurements of three quasi-compressional wave velocities within the symmetry planes at 45 degrees to the symmetry axes provide velocity surfaces for rocks with orthorhombic symmetry.

Velocities have been measured at 45 degrees to the symmetry axis for an Alpine schist sample (A-1) with axial symmetry [Godfrey *et al.*, 2000]. To describe three-dimensional

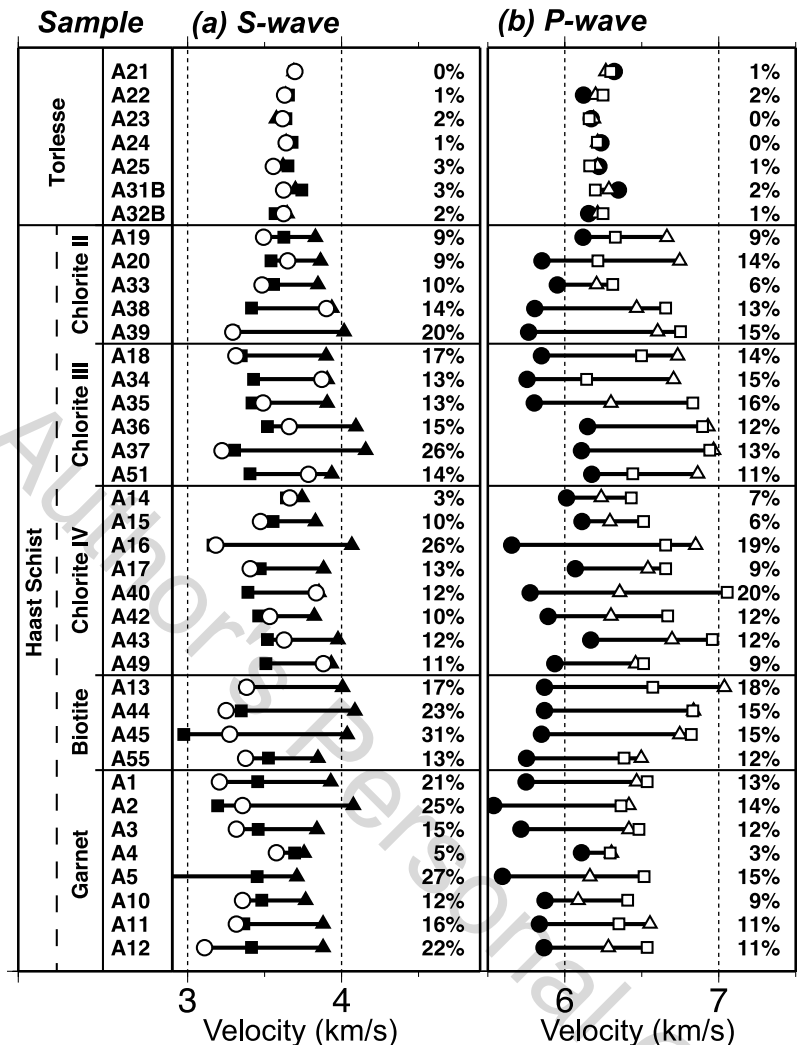


Figure 7. Velocities for Torlesse and Haast Schist metasedimentary rocks illustrating seismic anisotropy. Shear wave velocities (a) and compressional wave velocities (b) are at 600 MPa. For S-waves (a), open circle denotes propagation normal to foliation, solid square is vibration direction normal to foliation, and solid triangle is propagation and vibration parallel to foliation. For P-waves (b), solid circle denotes propagation normal to foliation, open triangle is propagation parallel to foliation but normal to lineation, and open square is propagation parallel to foliation plus lineation. Percent anisotropy is calculated from maximum velocity minus minimum velocity divided by the average of the three orthogonal velocities. Descriptions of the rock samples are provided in Tables 1–3.

wave propagation in this rock, phase velocity surfaces were calculated using the Kelvin–Christoffel equations [e.g., Auld, 1990] and elastic constants of the schist determined from the velocity and density measurements [Okaya and Christensen, 2002]. These surfaces (Figure 8) describe variations in phase velocity as a function of angle to foliation. Three velocity surfaces are calculated, one for the quasi-compressional wave (V_p), one for the shear wave vibrating parallel to the foliation (V_{sh}) and one for the quasi-shear wave vibrating in a plane perpendicular to the foliation (V_{sv}). For propagation

parallel and perpendicular to the foliation all wave modes are pure.

The velocity surfaces in Figure 8 show several interesting features about elastic wave propagation in the Alpine schist. First, compressional wave velocity does not increase significantly until propagation directions greater than about 40 degrees from foliation normal are reached. At an angle greater than 50 degrees compressional wave velocity increases rapidly and reaches a maximum for propagation parallel to the foliation. Shear wave singularities occur for propagation

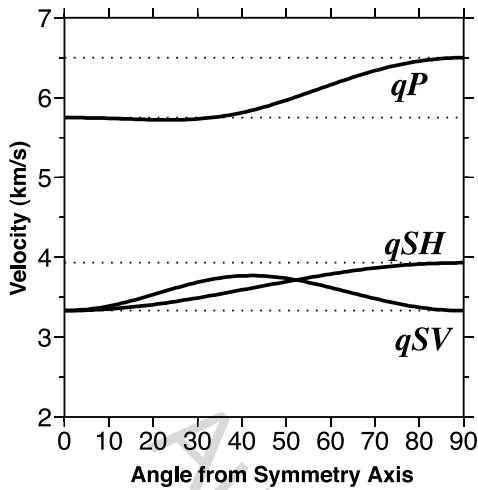


Figure 8. Phase velocities of the Haast schist as a function of angle from the symmetry axis normal to the foliation plane. The quasi-shear waves have equal velocity at approximately 50 degrees. Detectable shear wave splitting requires propagation at approximately 70–90 degrees from the symmetry axis (within 20 degrees of the foliation plane).

parallel to and at approximately 50 degrees to the symmetry axis (normal to the foliation). Although shear wave splitting occurs for all other propagation directions it does not exceed 0.2 km/s until propagation directions are greater than 65–70 degrees from the symmetry axis. Seismic sampling through this optimal but narrow range of propagation angles is made more difficult where geological structures exhibit 3D heterogeneity in the orientations of its internal fabrics [Okaya and Christensen, 2002]. Outside of this narrow range of propagation angles, the minimal production of shear wave splitting may misleadingly appear as isotropic seismic signals even though the schist material is strongly anisotropic. Thus field observations of crustal anisotropy by shear wave splitting will be difficult to observe unless the propagation direction is favorably oriented with respect to foliation (i.e., approximately parallel to foliation).

Significant measured material anisotropy in schist samples suggest that anisotropic signatures should be present in seismic data collected above the Haast schist terrane. While upper mantle anisotropy has been identified using Pn phases within SIGHT data [e.g., Scherwath *et al.*, 2002; Ballock and Stern, 2005; Bourguignon *et al.*, 2007, this volume], observations of crustal seismic anisotropy are difficult to identify [see Savage *et al.*, this volume]. Pulford *et al.* [2003] found limited evidence of shear wave splitting in SIGHT seismic onshore-offshore data collected within the Southern Alps. Stern *et al.* [2001] examined the role of schist anisotropy to produce

P-wave traveltimes within the Alpine fault zone before attributing the delays as due to elevated fluid pressures.

Because the production of a seismic anisotropic signal is directly dependent on the relative angles between the seismic wavepath and the material symmetry axes encountered along the full path, the three dimensional complexity of the Haast terrane internal structure is a contributing factor to whether the schist produces detectable seismic anisotropy. This complexity exists on three scales. At the broadest scale, in map view the Haast terrane is oroclinally bent by dextral 90 degrees as it approaches the Alpine fault (Plate 1). On a vertical crustal scale, geological models across central South Island suggest a subhorizontal Haast terrane which becomes upturned at the Alpine fault due to convergent exhumation and erosion – the “Wellman model” [Adams, 1979; Wellman, 1979; see Cox and Sutherland, this volume]. However, the orientation of the internal material fabric within this subhorizontal-to-upturning terrane is not well constrained and may be (a) internally subhorizontal or subvertical and (b) reoriented during exhumation by the mechanism of exhumation (e.g., “Wellman” upturning versus a backshear escalator [Little *et al.*, 2002, this volume]). These superimposed scales of geometrical complexity define the local and bulk regional orientation patterns of schist fabrics and hence influence the amount of seismic anisotropy which may be accumulated within seismic data.

The SIGHT experiments were not originally designed to collect seismic anisotropy. Onshore cross lines above the schist terrane were not collected orthogonal to the two main transects; analyses cannot be made to identify differences in schist-penetrating Pg velocities in perpendicular directions within the Southern Alps, eastern foothills, or (Canterbury) coastal plains. The deployment of three-component instruments during SIGHT were concentrated in the Southern Alps. Offshore seismic airgun signals and widely spaced explosion sources recorded by these instruments have raypaths with a more limited range of angles relative to local (and not well-constrained) schist fabric orientation. The SAPSE experiment did not employ dense transect or areal arrays across central South Island. Regional velocity structures obtained using isotropic seismic tomography methods [e.g., Eberhart-Phillips and Bannister, 2002] may have inherent larger uncertainties, necessitating the need for anisotropic tomography approaches [e.g., Eberhart-Phillips and Henderson, 2004]. In addition, high spatial resolution short period receiver function studies which are sensitive to crustal anisotropy have yet to be performed in central South Island within the Haast terrane.

The one set of seismic observations which was designed specifically as an attempt to observe schist seismic anisotropy was a SIGHT piggyback marine experiment in the

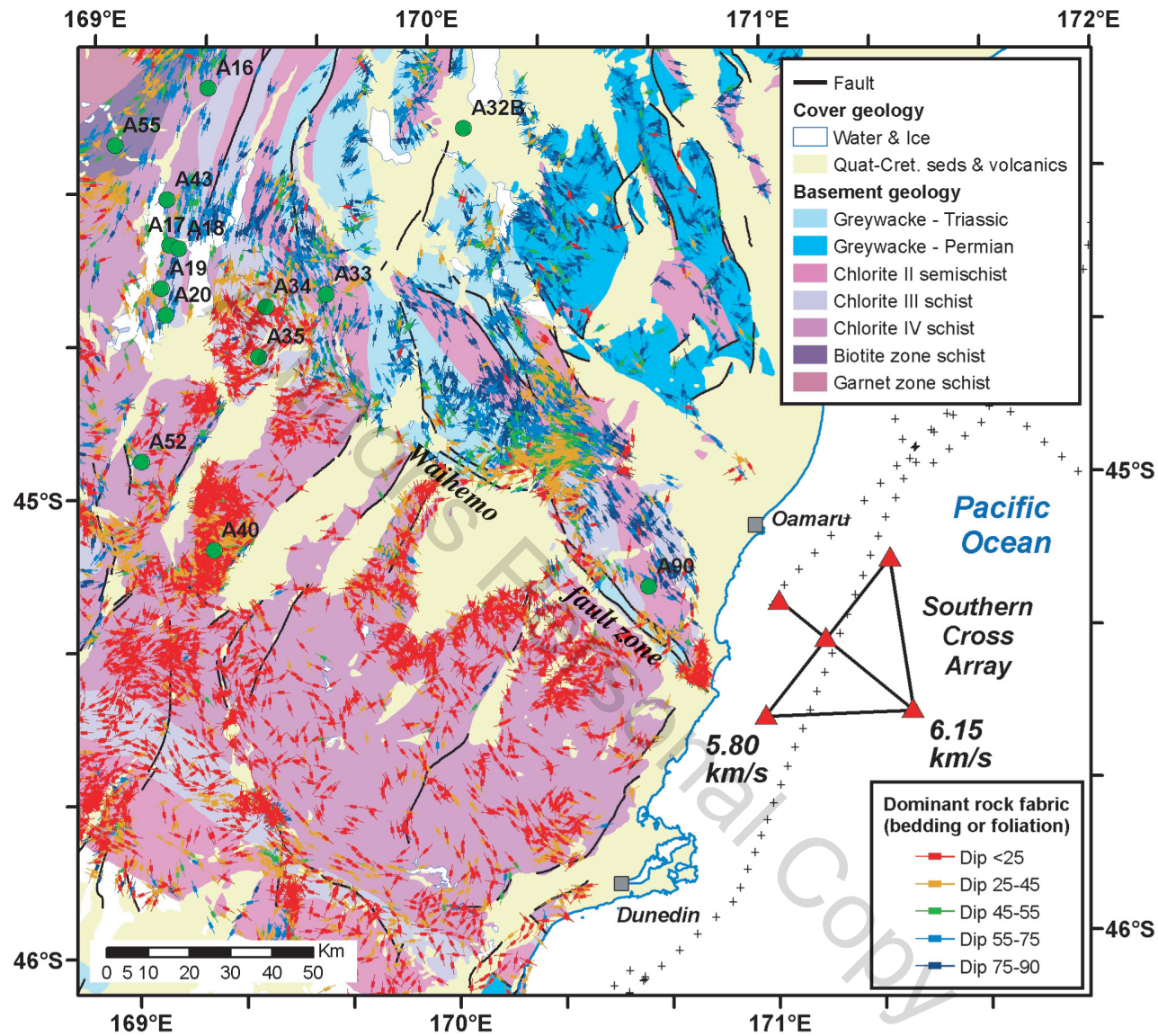


Plate 2. Location of Southern Cross seismic anisotropy experiment. Triangles denote locations of ocean bottom seismometers; solid lines connecting seismometer locations are seismic airgun ship tracks. Dominant rock fabric (schistosity) is sub-horizontal to gently dipping (warm color dip bars) for the Otago portion of the Haast schist southwest of the Waihemo fault zone and near-vertical (cool color dip bars) for the lower grade Torlesse greywacke and semischist further to the north. Labeled velocities represent upper crustal schist Pg velocities parallel to regional bulk foliation (6.15 km/s) and perpendicular (5.80 km/sec). Green circles are locations of rock samples as described in Tables 1–3. Lines of crosses denote SIGHT marine ship tracks. Geology map compiled from *Bishop and Turnbull [1996]*, *Turnbull [2000]*, *Forsyth [2001]*, and *Cox and Barrell [in press]* and was extracted from QMAP 1:250,000 geological map of New Zealand, courtesy of Simon Cox.

Pacific Ocean south of Oamaru. Nicknamed the “Southern Cross” due to its seismic array configuration, this experiment was positioned at the offshore extension of the Otago portion of the Haast schist (Plate 2). Land exposures near the coastline indicate this schist’s bulk foliation projects under the marine experiment with regional oriented NW to NNW strike and steep to vertical dips [Mutch, 1975; Cox and Sutherland, this volume]. Geologic field observations of this regional trend are denoted in Plate 2 (cool colored symbols). In contrast, southwest of the nearby Waihemo fault zone the schist defines a region of markedly differing schist foliation orientation. This latter portion of schist forms a structural northwest-trending anticlinorium with subhorizontal to moderate foliation dips (red symbols) [Cox and Sutherland, this volume]. The Waihemo fault zone clearly separates these domains of different rock fabric. The Southern Cross array used five ocean bottom seismometers to collect orthogonal reversed seismic refraction profiles using R/V *Ewing* airgun sources as deployed for SIGHT marine profiling. One refraction profile was approximately parallel to the regional schist foliation strike (NW-SE); its orthogonal profile is thus perpendicular to the regional foliation (Plate 2). Smith [1999] performed raytrace forward modeling of refracted and reflected P-waves and determined that upper crustal Pg phases penetrated the Haast schist basement at depths of approx. 5 km. Velocity analysis of these data defined P-wave velocities of 6.15 and 5.80 km/s along the profiles parallel and perpendicular to the bulk foliation strike, respectively. This represents P-wave seismic anisotropy of 5.9%. Smith [1999] conducted a reliability test to conclude that the difference in P-wave velocities was due to schist anisotropy and not due to unrelated factors such as phase mis-identification, travel time picking errors, or inversion parameter searches. The ability of a targeted seismic experiment to observe seismic anisotropy caused by schists suggests that a future combined passive- and active-source experiment design using azimuthal arrays may succeed in providing information about the subsurface schist’s structure and internal fabric characteristics. This information may provide constraints to tectonic or geodynamic models which describe Pacific plate upper and middle crustal deformation paths during transpressional exhumation at the Alpine fault plate boundary [e.g., Gerbault et al., 2002; Upton and Koons, this volume]

CONCLUSIONS

Laboratory measurements of the velocities of elastic waves to confining pressures of 1000 MPa for a variety of South Island, New Zealand rocks provide a comprehensive database for future interpretations of seismic velocities in

terms of petrology. The most useful velocities for this purpose are those measured at sufficiently high pressures to close grain boundary microcracks. Velocities in the pressure range of 100 to 300 MPa for Torlesse greywacke are consistent with shallow crustal seismic measurements over exposures of Torlesse. To the northeast of the Alpine fault zone crustal velocities of 6.2 to 6.4 km/s correlate with laboratory measurements of the Haast Schist Group. It is shown that the various subfacies of the Haast have similar velocities, so it is impossible to discern metamorphic grade of these rocks from seismic field experiments. Compressional wave velocities do however show a significant lowering with increasing iron content expressed in terms of Mg#. Propagation of seismic waves in the Haast Schist Group is further complicated by strong anisotropy expressed as compressional wave azimuthal variations and shear wave splitting. Future field experiments designed specifically to measure this anisotropy will be valuable for the determination of rock composition and structure of the New Zealand crust. This is a frontier research area that is certain to provide new and exciting insights into crustal structural geology.

Recent seismic velocity studies across central South Island [e.g., Eberhart-Phillips, 1995; Smith et al., 1995; Leitner et al., 2001; Scherwath et al., 2003; van Avendonk et al., 2004] have found the existence of a relatively high velocity basal layer with a thickness of 5 to 11 km and a compressional wave velocity of 6.7 to 7.3 km/s. These velocities are higher than most metasedimentary rocks of the Haast Schist Group, even if anisotropy is taken into account (Table 2, Figure 7). It has been suggested that this high velocity layer represents former oceanic crust [e.g., Holbrook et al., 1998], which is consistent with the layer thickness. If this layer is indeed oceanic crust, it is unlikely that original crustal lithologies (e.g., pillow basalts and sheeted diabase dikes) are now preserved. Rheological models of the Southern Alps predict that high shear strains propagate into the ductile lower crust during mountain building [e.g., Gerbault et al., 2002]. These shear strains will promote recrystallization resulting in strong foliations. Amphibolite facies mafic rocks, such as A-41 (average V_p = 7.01 km/s at 800 MPa) and A-53 (average V_p = 7.16 km/s at 800 MPa), are likely to be stable at depths of 25 to 35 km [e.g., Grapes, 1995]. Note that both samples show significant compressional and shear wave anisotropy, which is common in amphibolites [Christensen and Mooney, 1995], suggesting that in addition to the overlying crust this lower crustal seismic layer may also be anisotropic.

Acknowledgements. This study was supported by NSF grants EAR-9219496 and EAR-9418530. We thank Simon Cox who generated the geological map of eastern South Island using the digital QMAP 1:250,000 Geological map of New Zealand. We thank

Ryan Smith and W. Steven Holbrook for fruitful discussions regarding offshore seismic anisotropy. Tom Brocher and an anonymous reviewer provided excellent comments. We also thank Sabrina Bradshaw and Anna Coutier for their assistance in assembling the petrophysical laboratory tables that are also provided in digital form in the CDROM which accompanies this volume.

REFERENCES

- Adams, C. J. D. (1979), Age and origin of the Southern Alps, in *The Origin of the Southern Alps, R. Soc. N. Z. Bull.*, vol. 18, edited by R. I. Walcott and M. M. Cresswell, pp. 73–78.
- Auld, B. A. (1990), *Acoustic Fields and Waves in Solids*, vol. 1, Robert E. Krieger, Malabar, FL, 435 pp.
- Baldock, G., and T. Stern (2005), Width of mantle deformation across a continental transform: evidence from upper mantle (Pn) seismic anisotropy measurements, *Geology*, 33, 741–744.
- Birch, F., (1960), The velocity of compressional waves in rocks to 10 kilobars, 1, *J. Geophys. Res.*, 65, 1083–1102.
- Birch, F. (1961), The velocity of compressional waves in rocks to 10 kilobars, 2, *J. Geophys. Res.*, 66, 2199–2224.
- Bishop, D. G., J. D. Bradshaw, and C. A. Landis (1985), Provisional terrane map of South Island, New Zealand, in *Tectonostratigraphic Terranes*, edited by D. G. Howell, Circum-Pacific Council for Energy and Mineral Resources, Houston, TX, pp. 515–521.
- Bishop, D. G. and I. M. Turnbull (1996), *Geology of the Dunedin area, Institute of Geological & Nuclear Sciences 1:250,000 geological map 21 Scale 1:250,000*, Institute of Geological and Nuclear Sciences, Lower Hutt, New Zealand, 1 sheet + 52 pp.
- Bourguignon, S., T. Stern, and M. K. Savage (2007), Crust and mantle thickening beneath the southern portion of the Southern Alps, New Zealand, *Geophys. J. Int.*, 168, 681–690.
- Bourguignon, S., M. K. Savage, and T. Stern (this volume), Crustal thickness and Pn anisotropy beneath the Southern Alps oblique collision, New Zealand.
- Brocher, T. M. (2005), Empirical relations between elastic wavespeeds and density in the Earth's crust, *Bull. Seismol. Soc. Am.*, 95, 2081–2092.
- Brocher, T. M., M. A. Fisher, E. L. Geist, and N. I. Christensen (1989), A high resolution seismic reflection/refraction study of the Chugach-Peninsular terrane boundary, southern Alaska, *J. Geophys. Res.*, 94, 4441–4555.
- Christensen, N. I. (1965), Compressional wave velocities in metamorphic rocks at pressures to 10 kbar, *J. Geophys. Res.*, 70, 6147–6164.
- Christensen, N. I. (1966), Shear wave velocities in metamorphic rocks at pressures to 10 kilobars, *J. Geophys. Res.*, 71, 3549–3556.
- Christensen, N. I. (1996), Poisson's ratio and crustal seismology, *J. Geophys. Res.*, 101, 3139–3156.
- Christensen, N. I., and W. D. Mooney (1995), Seismic velocity structure and composition of the continental crust: A global view, *J. Geophys. Res.*, 100, 9761–9788.
- Christensen, N. I., and Szymanski (1988), Origin of reflections from the Brevard fault zone, *J. Geophys. Res.*, 93, 1087–1102.
- Cox, S. C., and D. J. A. Barrell (in press), *Geology of the Aoraki area, Institute of Geological and Nuclear Sciences 1:250,000 geological map 15*, Institute of Geological and Nuclear Sciences, Lower Hutt, New Zealand, 1 sheet + 71 pp.
- Cox, S. C., and R. Sutherland (this volume), Regional geological framework of South Island, New Zealand, and its significance for understanding the active plate boundary.
- Davey, F. J., T. Henyey, W. S. Holbrook, D. Okaya, T. Stern, A. Melhuish, S. Henrys, D. Eberhart-Phillips, T. McEvilly, R. Urhammer, H. Anderson, F. Wu, G. Jiracek, P. Wannamaker, G. Caldwell, and N. Christensen (1998), Preliminary results from a geophysical study across a modern continent-continent collisional plate boundary—the Southern Alps, New Zealand, *Tectonophysics*, 288, 221–235.
- Davey, F. J., D. Eberhart-Phillips, M. D. Kohler, S. Bannister, G. Caldwell, S. Henrys, M. Scherwath, T. Stern, and H. van Aenddonk (this volume), Geophysical structure of the Southern Alps orogen, South Island, New Zealand.
- Eberhart-Phillips, D. (1995), Examination of seismicity in the central Alpine fault region, South Island, New Zealand, *N. Z. J. Geol. Geophys.*, 38, 571–578.
- Eberhart-Phillips, D., and S. Bannister, (2002), Three-dimensional crustal structure in the Southern Alps region of New Zealand from inversion of local earthquakes and active source data, *J. Geophys. Res.*, doi:10.1029/2001JB000567.
- Eberhart-Phillips, D., and M. Henderson, (2004), Including anisotropy in 3-D velocity inversion and application to Marlborough, New Zealand, *Geophys. J. Int.*, 156, 237–254.
- Forsyth, P. J. (2001), *Geology of the Waitaki area, Institute of Geological and Nuclear Sciences 1:250,000 geological map 19*, Institute of Geological and Nuclear Sciences, Lower Hutt, New Zealand, 1 sheet + 64 pp.
- Frost, C. D., and D. S. Coombs (1989), Nd isotope character of New Zealand sediments: Implications for terrane concepts and crustal evolution, *Am. J. Sci.*, 289, 744–770.
- Fuis, G. S., et al. (1991), Crustal structure of accreted terranes in southern Alaska, Chugach Mountains and Copper River Basin from seismic refraction results, *J. Geophys. Res.*, 96, 4187–4227.
- Gerbault, M., F. Davey, and S. Henrys (2002), Three-dimensional lateral crustal thickening in continental oblique collision: an example from the Southern Alps of New Zealand, *Geophys. J. Int.*, 150, 770–779.
- Godfrey, N. J., N. I. Christensen, and D. A. Okaya (2000), Anisotropy of schists: contribution of crustal anisotropy to active source seismic experiments and shear wave splitting observations, *J. Geophys. Res.*, 105, 27,991–28,007.
- Godfrey, N. J., N. I. Christensen, and D. A. Okaya (2002), The effect of crustal anisotropy on reflector depth and velocity determination from wide-angle seismic data: a synthetic example based on South Island, New Zealand, *Tectonophysics*, 355, 145–161.
- Grapes, R. H. (1995), Uplift and exhumation of Alpine schist, Southern Alps, New Zealand: thermobarometric constraints, *N. Z. J. Geol. Geophys.*, 38, 525–533.

- Holbrook, W. S., D. Okaya, T. Stern, F. Davey, S. Henrys, and H. van Avendonk (1998), Deep seismic profiles across the Pacific-Australian plate boundary, South Island, New Zealand, *Eos Trans. AGU*, 79, F901.
- Hughes, S., J. H. Luetgert, and N. I. Christensen (1993), Reconciling deep seismic refraction and reflection data from the Grenvillian-Appalachian boundary in western New England, *Tectonophysics*, 225, 255–269.
- Iida, K., T. Sugio, H. Furuhashi, and M. Kumazawa (1967), Elastic wave velocity in crystalline Schists from Sanbagawa metamorphic terrane, Shikoku, Japan, *J. Earth Sci. Nagoya Univ.*, 15, 112–123.
- Ji, S., and M. H. Salisbury (1993), Shear wave velocities, anisotropy and splitting in high-grade mylonites, *Tectonophysics*, 221, 453–473.
- Johnston, J. E., and N. I. Christensen (1995), Seismic anisotropy of shales, *J. Geophys. Res.*, 100, 5991–6003.
- Kern, H., and H.-R. Wenk (1990), Fabric related velocity anisotropy and shear wave splitting in rocks from the Santa Rosa mylonite zone, California, *J. Geophys. Res.*, 95, 11,212–11,223.
- Landis, C. A., and D. S. Coombs (1967), Metamorphic belts and orogenesis in southern New Zealand, *Tectonophysics*, 4, 501–518.
- Leitner B., D. Eberhart-Phillips, H. Anderson, and J. L. Nabelek (2001), A focused look at the Alpine fault, New Zealand: seismicity, focal mechanisms, and stress observations, *J. Geophys. Res.*, 106, 2193–2220.
- Little, T. A., R. J. Holcombe, and B. R. Ilg (2002), Ductile fabrics in the zone of active oblique convergence near the Alpine Fault, New Zealand: identifying the neotectonic overprint, *J. Struct. Geol.*, 24, 193–217.
- Little, T., R. Wightman, R. J. Holcombe, and M. Hill (this volume), Transpression models and ductile deformation of the lower crust of the Pacific Plate in the central Southern Alps, a perspective from structural geology.
- Miller, D. J., and N. I. Christensen (1994), Seismic signature and geochemistry of an island arc: a multidisciplinary study of the Kohistan accreted terrane, northern Pakistan, *J. Geophys. Res.*, 99, 11,623–11,642.
- Mutch, A. R. (1975), *Geological map of New Zealand 1:250,000, sheet 23: Oamaru*, Dept. Sci. Ind. Res., Wellington, New Zealand.
- O'Connell, R. J., and B. Budiansky (1974), Seismic velocities in dry and saturated cracked solids, *J. Geophys. Res.*, 79, 5412–5426.
- Okaya, D., N. I. Christensen, D. Stanley, and T. S. Stern (1995), Crustal anisotropy in the vicinity of the Alpine Fault Zone, *N. Z. J. Geol. Geophys.*, 38, 579–583.
- Okaya, D., and N. I. Christensen (2002), Anisotropic effects of non-axial seismic wave propagation in foliated crustal rocks, *Geophys. Res. Lett.*, doi:10.1029/2001GL014285.
- Pulford, A., M. Savage, and T. Stern (2003), Absent anisotropy: the paradox of the Southern Alps orogen, *Geophys. Res. Lett.*, 30, 20, doi:10.1029/2003GLO17758.
- Savage, M., M. Duclos, and K. Marson-Pidgeon (this volume), Seismic anisotropy in South Island, New Zealand.
- Scherwath, M., A. Melhuish, T. Stern, and P. Molnar (2002), Pn anisotropy and distributed upper mantle deformation associated with a continental transform fault, *Geophys. Res. Lett.*, doi:10.1029/2001GL014179.
- Scherwath, M., T. Stern, F. Davey, D. Okaya, W. S. Holbrook, R. Davies, and S. Kleffmann, (2003), Lithospheric structure across oblique continental collision in New Zealand from wide-angle P-wave modeling, *J. Geophys. Res.*, 108, 2566, doi:10.1029/2002JB002286.
- Smith, E. G. C., T. Stern, and B. O'Brien (1995), A seismic velocity profile across the central South Island, New Zealand, from explosion data, *N. Z. J. Geol. Geophys.*, 38, 565–570.
- Smith, R. A. (1999), Macroscopic P-wave anisotropy in the Haast Schist, New Zealand: implications for errors in wide-angle seismic studies of metamorphic terranes, Masters thesis, University of Wyoming, Laramie, WY, 147 pp.
- Stern, T., S. Kleffmann, D. Okaya, M. Scherwath, and S. Bannister (2001), Low seismic-wave speeds and enhanced fluid pressure beneath the Southern Alps of New Zealand, *Geology*, 29, 679–682.
- Turnbull, I. M. (2000), Geology of the Wakatipu area, Institute of Geological and Nuclear Sciences 1:250,000 geological map 18. Lower Hutt, Institute of Geological and Nuclear Sciences Ltd. 1 sheet + 72 p.
- Upton, P., and P. O. Koons (this volume), Three-dimensional geodynamic framework for the Central Southern Alps, New Zealand: integrating geology, geophysics and mechanical observations.
- Stewart, R. and L. Peselnick (1977), Velocity of compressional waves in dry Franciscan rocks to 8 kilobar and 300°C, *J. Geophys. Res.*, 82, 2027–2039.
- van Avendonk, H. J. A., W. S. Holbrook, D. Okaya, J. K. Austin, F. Davey, and T. Stern (2004), Continental crust under compression: a seismic refraction study of South Island Geophysical Transect I, South Island, New Zealand, *J. Geophys. Res.*, 109, B06302, doi: 10.1029/2003JB002790.
- Wellman, H. W. (1979), An uplift map for the South Island of New Zealand, and model for the uplift of the Southern Alps, in *The Origin of the Southern Alps*, R. Soc. of N. Z. Bull., vol. 18, edited by R. I. Walcott and M. M. Cresswell, pp. 12–20.

N. I. Christensen, Department of Geology and Geophysics, University of Wisconsin-Madison, Madison, WI, USA.

D. A. Okaya, Department of Earth Sciences, University of Southern California, Los Angeles, CA, USA.

Author's Personal Copy